Part 1: Phase 1 Final Report for

TPF Pre-Formulation Phase Study

1 April 2002

In response to:

Terrestrial Planet Finder Contract 1217283
Jet Propulsion Laboratory
4800 Oak Grove Drive
Pasadena, CA 91109

Submitted by:

Lockheed Martin Space Systems Company
Missiles & Space Operations
1111 Lockheed Martin Way
Sunnyvale, CA 94089

Table of Contents

5.1.1 Lockheed Martin Team

5.1.1.1 Approach

Study Summary

Objectives & process

The task of Phase 1 of the TPF Pre-Formulation Phase Study was to perform trade studies of a diverse set of architecture options. The overall objective of the Lockheed Martin team was to determine the optimum engineering approach for affordably meeting the JPL-provided science requirements for terrestrial planet detection and characterization. The selected architectures were developed with respect to science requirements provided by JPL and evaluated using JPL-provided criteria. Astrophysical research capabilities were assessed for each architectural option.

Meeting this objective involved developing and defining a rational set of architectures. These were referred to as "Islands of Sanity". Five "Islands" were identified and characterized, which provided a realistic technology solution for achieving the science requirements. These were:

Island 1: Separate Spacecraft Interferometer (SSI) (Free Flyers)

Island 2: Segmented Mirror Interferometer (SMI)

Island 3: Structurally Connected Interferometer (SCI)

Island 4: Tethered Spacecraft Interferometer (TSI)

Island 5: Coronagraph

The Lockheed Martin team performing these studies consisted of science and engineering personnel from Lockheed Martin Missiles & Space in Sunnyvale, the University of Arizona Steward Lab, MIT, and Busek Engineering. The study team was under the direction of Dr. Domenick J. Tenerelli, Lockheed Martin Division of Remote Sensing and Space Sciences. Responsibilities for Phase 1 and the study plan are shown in Figure 1-1.

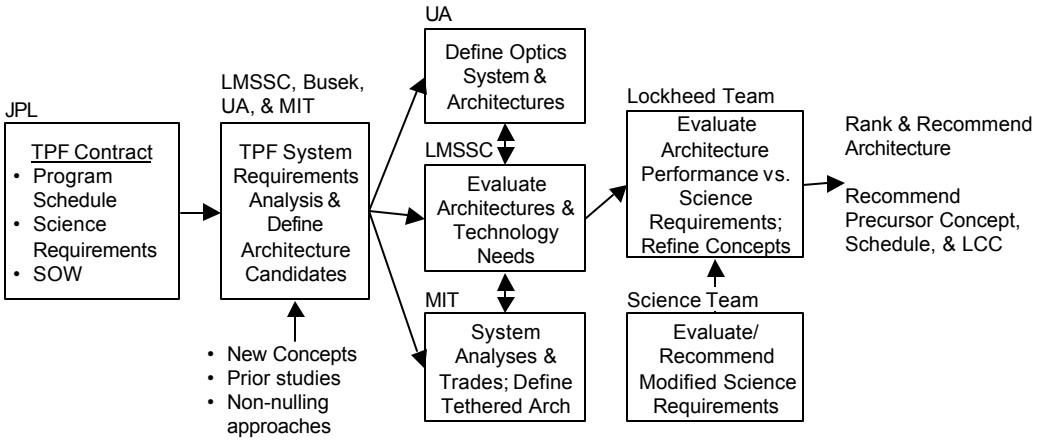

Figure 1-1: Lockheed Martin Phase 1 study plan

A step-by-step evaluation process was used to provide the ranking of the various architectures. The process involved identification of architecture candidates, development of optics system concepts, development of candidate architectures, trades, analyses, assessments of performance

against JPL-provided criteria, and determination of life cycle cost (LCC). The process is shown in Figure 1-2.

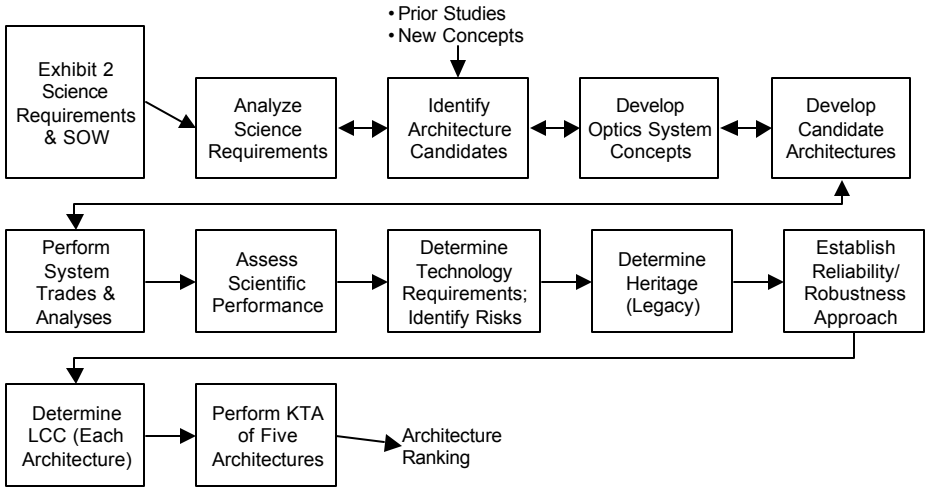

Figure 1-2: Architecture study process

Evaluation of candidate architectures was accomplished using the Kepner-Tregoe Analysis (KTA) approach. We implemented a rigorous system engineering process that systematically considered significant features of each architectural configuration. The team met on a regular basis throughout Phase 1. An offsite meeting of 3 1/2 days duration was held to kick off the study effort. A total of seven team meetings were held at rotating locations of Sunnyvale, Tucson, and Cambridge. The final KTA evaluation was held during a one week team meeting at LMSSC-Sunnyvale. Evaluation criteria included planetary detection, astrophysics opportunities, technology requirements, risk, LCC (Phase BCD), reliability/robustness, and heritage (legacy). Each criterion was weighted on a scale 1–10. The candidate architectures were then assessed with respect to each other for each criterion and scored. A weighted score was then developed as the product of the relative score and the criterion weight. A sum total was then determined for each of the configurations ("Islands"). The architectures were then ranked. Program schedules were developed for the recommended architectures to support determination of LCC.

We determined that a precursor mission approach would be of significant benefit in reducing TPF program risk while providing an early demonstration of technology in flight and yielding important science data on planet detection.

Science Requirements

Planetary Systems

We first reviewed the proposed science goals for terrestrial planets, because these are the defining goals for the existence of the program. We considered the potential environments of terrestrial planets, and asked whether the earth is likely typical of a planet of its size in its particular radiative environment. The principal doubt arises whether the volatile materials present on earth (carbon, hydrogen, oxygen, nitrogen, and sulfur), which are also the key constituents of living matter, were deposited on earth as part of the matter at 1 AU coming together, or whether they were provided by meteoritic or cometary material especially directed into the inner solar system as a result of orbital perturbations by giant planets. For this reason we argued that a crucial as-

pect of TPF is that it should also be able to characterize the planetary systems in which earth-like planets are found, and determine the presence or absence of giant planets.

Also, we reviewed an analysis of the process of formation and spiralling inward of giant planets (Lunine and Trilling). This study suggested that there are large selection effects in the discovery of giant planets. It is expected that planetary systems are much more common than current observations suggest (~5%), and that planets in large orbits are about three times as common as those that spiral inward, and have been found by radial velocity measurements. This result encourages us to believe that planetary systems like our own are relatively abundant, present around perhaps one star in 3 or 4, and that a smaller, cheaper TPF mission would have a good probability of finding earth-like planets. We therefore also focussed a substantial part of our effort in looking for ways to reduce the cost and increase the speed of a TPF mission.

Spectral Signatures

Next we examined the spectral regions for an indication of which would provide appropriate information for a TPF mission. Our conclusions were that only two spectral regions provided good information about the temperature and size of an earth-like planet and that these are the mid-IR and millimeter waves. The mm-wave spectrum can measure the earth temperature and size, the abundance of water vapor (13.5 mm) and the abundance of oxygen (5.5 mm). We can estimate the required telescope sizes, based on fundamental noise limits of receivers in this spectral region, and unfortunately they need to have diameters of kilometers. Therefore we turned to the mid-IR. Here we found that much smaller devices could measure the planet size and temperature, and also detect ozone (which is an easier to detect variant of oxygen), carbon dioxide (which also measures the presence or absence of a thermal inversion at a tropopause), and water vapor. Quantitative abundance determinations are difficult in the mid-IR, but the ozone band in particular is extremely sensitive to even a very small abundance of oxygen in an atmosphere.

For the visible spectral region we have been able to find only one good temperature indicator for earth: the presence of the vegetation edge! Thus if life has produced land vegetation like that of earth, we can recognize it, but if it has not, we do not know what the size and temperature are for the planet. And then we are unable to interpret band strengths in terms of abundances. We regard the infrared spectrum as more desirable as a starting point than the visible spectrum, but clearly the combination of the two would be much better than either alone.

We also examined the nearer IR spectrum. Again we found no temperature indicators. Water vapor is easier to see in the 1–2 μm region than in the visible. Carbon dioxide shows at 2.06 μm and 4.3 μm. But the 1.2 μm oxygen band is weaker than the A-band in the visible. There is a cleanly separate methane band at 3.3 μm, but that is near the spectral crossover between absorption and emission. It is comparable in difficulty with detection of the 7.65 μm methane band, which though stronger, has confusing N_2O and water absorption in its spectral region. We concluded that the wavelength regions in order of decreasing science value for a first flight are mm-wave : mid-IR : optical : near-IR. However, the mm-wave mission is found to be totally impractical for the 21st century. This leaves the mid-IR as the preferred region, with the visible region also having a high priority.

Planet Detection

We developed some numbers associated with the technical requirements for observing planets. First we studied the star to planet contrast, shown in Table 1-1. Note the rapid change of star-to-planet ratio from 7 µm to 20 µm. Also note that the fluctuation of residual star signal must be reduced to allow high signal-to-noise for planet observations. However, the local zodiacal flux is brighter than the planet. It is not necessary to reduce the star flux to that of the planet, but only so that it ceases to dominate the total received signal. The effect of the change of star to planet ratio from 10 µm to 7 µm is that observations of ozone at 9.6 µm will provide a much better SNR than the detection of methane at 7.65 µm.

Table 1-1: Star-to-planet contrast

Wavelength	Contrast
0.5-4 µm	5×10^9
7 µm	10^8
10 µm	1.2×10^7
20 µm	1.7×10^6
10 mm	2×10^5

Now the local zodiacal flux will provide a constant signal regardless of the telescope size, so the reduction of star flux as specified above needs to be greater if the star is closer and brighter. But in fact most of the stars will be at almost the greatest distance (because the numbers increase as distance cubed), so the overall time will not change much if we push the nulling ratio so that only the more distant stars have local zody dominant.

Contrast between star and local zody varies with star distance and telescope aperture size. Here we consider the star to be at 16 pc, observed with a set of four equal-sized telescopes and consider the flux within the star diffraction core. These numbers define a lower limit to the nulling factor needed at each wavelength. The ratio of these numbers to the star-planet ratio define the contrast with which the local zodiacal flux will be seen above the planet.

Table 1-2: Nulling requirements

Wavelength	4 × 3.5 m telescopes	4 × 2.5 m telescopes	4 × 1.7 m telescopes
7 µm	9×10^5	4.5×10^5	2.3×10^5
10 µm	6×10^4	3×10^4	1.5×10^4
20 µm	2×10^3	1×10^3	5×10^2

For planets which are close, and which have a high zodiacal flux from their own system, the exozodiacal flux may exceed the local zodiacal flux. Thus, if our own planetary system were to be observed, we would find after nulling that the zodiacal flux was 200 times that of the earth, an approximately wavelength independent number from 7–30 µm.

Table 1-3: Ratio of exo-zody to star

Wavelength	4 × 3.5 m telescopes	4 × 2.5 m telescopes	4 × 1.7 m telescopes
7 µm	1.8	0.9	0.45
10 µm	1.0	0.5	0.25
20 µm	0.25	0.13	0.06

We then find that if we had this nulling, and the system were like the solar system, then the ratio of exo-zody to star would be as shown in Table 1-3. For the closest planetary systems, or brighter exozodiacal dust, the proposed level of nulling would be unnecessary. It can be seen that exozodiacal dust can become significant if:

a) One is trying to get much higher signal to noise on nearer planetary systems.

b) One is trying to benefit from using larger telescopes.

c) One is trying to observe systems in which the dust is relatively brighter than in the solar system, and in particular if one is also trying to benefit from (b) and (c).

Thus for close by planetary systems, exozodiacal dust will limit the benefit that might apparently be obtained by better nulling. Note also that for 4 x 2.5 m telescopes, even if the exozodiacal dust were 10 times brighter than in our solar system, for planetary systems at 16 pc, the observing time would only need to be increased by a factor 4, and for dust 3 times brighter, the factor is 1.7.

General Astrophysics

As we investigated the use of the interferometer for astrophysics, we came across certain severe problems. The field of view is given by the telescope diffraction pattern, and the resolution is given by the maximum mirror separation. The image should therefore be a number of pixels across equal to the mirror separation divided by the mirror size. For separation equal to 1 km, this value is about 300. The spectral resolution needed for the interferometer to be able to create a picture ~300 elements across is ~300. Therefore the device needs a high resolving power spectrograph as part of its use—quite different from the needs of planet finding in the mid-IR.

Next there is a problem of the large unfilled area of the *u-v* plane near the image center. These arise because there is a risk in bringing free-flying mirrors close together, and for a truss interferometer, the non-redundant spacing of mirrors needed for imaging is inconsistent with the highly redundant spacing needed for planet finding.

The effect of widely spaced mirrors is that the low spatial frequencies are not determined, and there is confusion as to where the parts of the image should be placed. In part this can be resolved if one assumes that the structure of the source has no highly frequency dependent parts. Then the use of adjacent frequency channels can remove some ambiguity, but in general, only the central part of the image is likely to be useable, unless the data are obtained with very high SNR.

One way of solving the problem is to make a truss interferometer the center of an astrophysical free-flying instrument. The truss instrument will then fill in all the high spatial frequencies, and the free-flying mirrors can fill in the rest.

For this reason, it is interesting to consider the use of a truss nuller to prepare for such an astrophysical instrument. And because some truss nuller mirrors can be moderately spaced, it is possible to bridge the gap to NGST resolution. Even a short truss interferometer could make observations that are several times the angular resolution of NGST, and of far higher sensitivity than is possible from the ground. Indeed the reduced background in space makes a space telescope at 10 μm perform with the sensitivity of a telescope ~30 times larger in diameter on the ground.

5.1.1.2 Concepts Investigated

Island 1: Separate Spacecraft Interferometer (Free Flyers)

The benefits of the free-flyer concept are increased mission flexibility and greater utilization of the *u-v* imaging plane because the spacecraft formation is re-configurable. The free-flyer concept

enables distributed apertures with longer baselines and greater fault tolerance. The free-flyer architecture is an integration of various technology concepts. Technologies required for TPF free-flyer architecture include design and modeling of distributed systems, inter-satellite communications, autonomy for distributed systems, distributed computing, coordination commanding and control of distributed spacecraft, distributed system fault tolerance, nano- or micro-propulsion, and power collection and distribution. Technology readiness, cost, and risk reduction requires design, analysis, and demonstration in the areas of command, attitude control, power, thermal, fault protection, communications, autonomy, and propulsion.

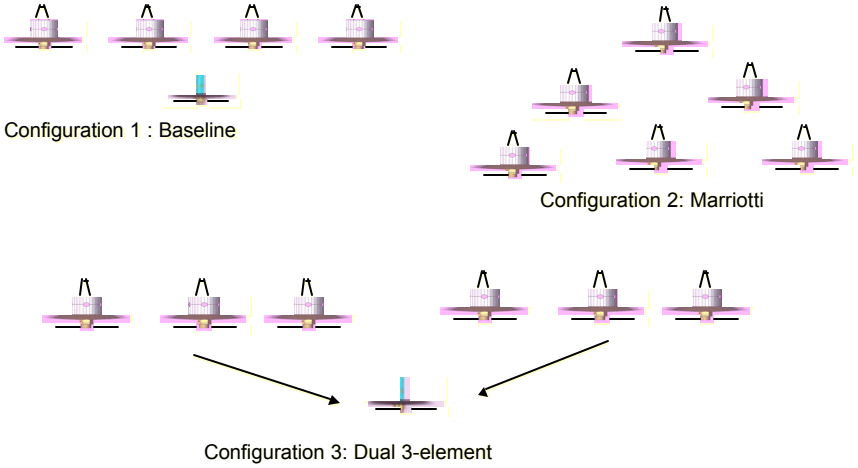

Figure 1-3: Separate spacecraft interferometer (free flyer) configurations

Flying spacecraft in formation necessitates the extension of the theory of formation flight control to allow for precision three-dimensional formation maneuvers. Thus, a navigation control algorithm was formulated for the TPF free-flyer architecture. The control algorithm is an eighteen-state signal control system that models the dynamics of multi-spacecraft formation in three-dimensional space. An LQG-decentralized automatic control system was designed to maintain the spacecraft in the specified formation geometry, and its performance was examined in simulation experiments. Performance results matched identically to a similar LQG-centralized formation control algorithm.

The concept of using navigation instrumentation as a communication device and a navigation device for TPF formation flyers was investigated. The expected bandwidth of the communication system is ~156 kbps. With short distances between TPF vehicles, substantially higher data rates should be achievable. The ranging techniques involve the transmission of short electromagnetic pulses via a current radiating antenna loop. These short pulse width signals have a very large signal bandwidth (~1–2 GHz). The goal is to achieve between 5 to 10 Mbps. By expanding the capacity of the system to 5–10 Mbps, all vehicle communication can potentially occur via the system. If the vehicle communicates in a multicast mode, additional bandwidth is not required for sending data to multiple vehicles. As of 2002, the navigation instrumentation has been tested in the Lockheed Martin facility and static measurement yielded ~3 cm accuracy, with a sub-cm theoretical limit. Dynamics measurement studies are proposed in our new indoor test bed.

Island 2: Segmented Mirror Interferometer

The initial concept was to have free-flying segments of a primary mirror, with the focus at a separate free-flying beam-combiner. This would avoid a potentially complex beam combining

system. In the interests of simplification we then put the mirror segments on to a truss, and allowed the possibility of the segments moving along the truss.

We found two problems associated with free-flying segments. First, that shielding segments from the sun and from one another was a major issue. Second, the precision of placement required for the beam combiner seemed excessively high.

Eventually we rejected this scheme on the grounds that for planet detection it did not offer any special advantages over a truss with a beam combiner on it, while offering a likelihood of considerably greater complexity, risk, and cost.

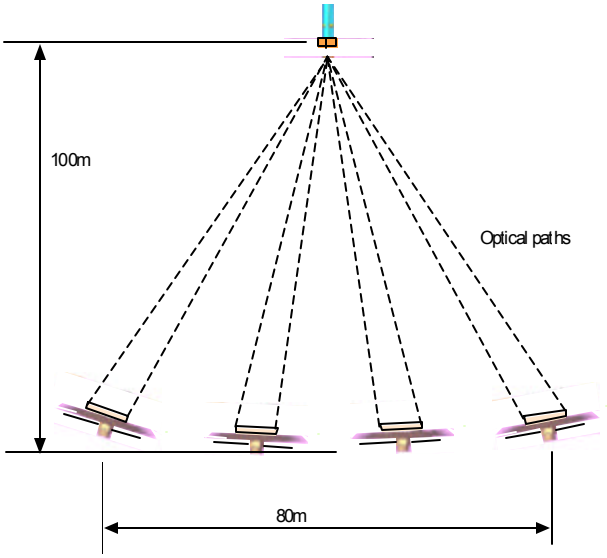

Figure 1-4: Segmented mirror interferometer

Island 3: Structurally Connected Interferometer

The connected structure was the first concept considered for TPF. Figure 1-5 shows a diagram of the configuration. The biggest problem was the large rigid truss: Able-mast type structures seemed excessively flimsy. Further, if we tried a folded truss, and made it very long, then the possible cross-section of the truss became small, and so it too became flimsy. For this reason at the PAR stage we considered the truss concept to likely be more expensive than free-flyers.

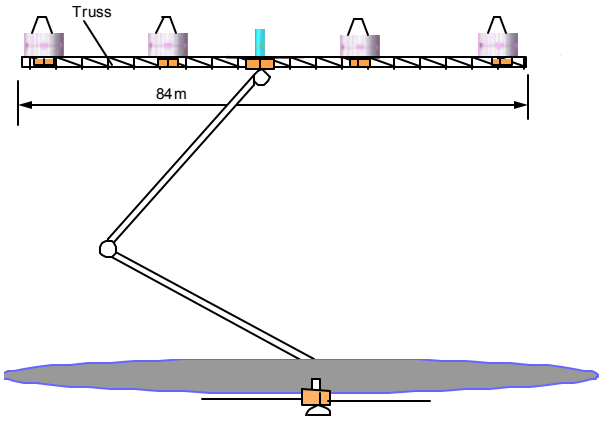

Figure 1-5: Structurally connected interferometer

At the PAR, we tried to configure the interferometer as a degenerate Angel Cross configuration, however the beam combining for that is very difficult, and so a further configuration was investigated during Phase II of the study. However, during this process we became alert to a set of possibilities that flowered in our final analysis stage. We began to investigate whether it was necessary to have a truss as long as had been initially proposed, 50–75 m. This length was largely driven by the outrigger mirrors, which contributed very little energy to the final image, but seemed needed to broaden the null. The broadened null seemed needed to reduce the sensitivity of the nulling to the telescope pointing and beam alignment.

However, in the earlier TPF book appendix, there was an analysis of the various terms that entered into the detection of a planet. The analysis showed that if the star was nulled to a factor between 10^{-4} and 10^{-5}, it ceased to contribute significant photon noise, and instead became a problem for potentially fluctuating as the nulling precision changed. However, the nulling phase signal is very bright, and so offers the opportunity for adequate control of variation. If a simple 2-beam interferometer were used, the fact that the null was not very good on a large angular diameter star became the only significant issue.

So we looked into interferometers where there was a possibility of two different baselines, one appropriate for large diameter stars, and the relatively widely separated planets they would have, and a second longer baseline appropriate for the more distant stars. We found that it was possible to combine two former variant ideas for TPF. The first concept was proposed by Shao, Velusamy and Beichman, and used two short baseline interferometers, of identical baseline, separated by a somewhat larger distance. This system was able to use its short baseline to null the star well, and its longer baseline to separate the planet from possibly bright exozodiacal dust.

The second configuration was suggested by Woolf and Angel. In it, two long baseline interferometers were interleaved, and used so as to distinguish whether the planet was to one side or the other of its star. The use of either of these interferometers required a two-stage beam combiner (as is needed for any interferometer with 3 or 4 mirrors). Both outputs show the presence of planets, but they do so at different places in the rotation. Therefore, if the phase is chopped for the second beam combining, so as to alternate the two outputs onto detectors, the difference signal reflects only planet signals, and removes any thermal drift. Further, since the first stage phase measurement can be used to stabilize the star leak, neither thermal nor phasing drift should affect the output. This concept had been published by Woolf, Angel, Beichman, Burge, Shao, and Tenerelli, in a study for a small folded nulling interferometer.

It is not possible to exactly configure the two concepts together. The Shao-Velusamy-Beichman concept when used at only moderate separations between the pairs requires certain ratios of separations to give a simple interferogram, and these do not match the Woolf-Angel ratios. However it was found that it is possible to operate the Woolf-Angel arrangement with a slightly more compressed format than proposed, with minimal effects on the brightness of the closest fringe. This therefore has become the format of the further investigations. The overall length is 1.4 times the wider spaced nulling length, and there is a ~0.5 intensity fringe inside the main fringe of the shorter baseline.

The benefits of this scheme can be seen quantitatively. The original 75 m and 50 m interferometers proposed for TPF had a minimum planet angular separation from the star at 10 μm of 0.055 and 0.037 arcsec for their closest fringe. To get the same resolution with an interleaved interferometer requires long baselines of 18.75 m and 28.12 m. With interleaving these give overall

interferometer lengths of 26.2 m and 39.4 m, or roughly half as long as the OASES scheme of Angel and Woolf. Whereas the packaging of a 75 m rigid truss is difficult and even a 50 m is not easy, difficulties are substantially reduced for 26 m or 40 m trusses.

We have found certain particular truss lengths appear to be significant in changing the difficulty of making a TPF. The longest unfolded truss that can fit into the currently available largest cold chamber is ~21 m. The longest truss that can be fitted with a single fold into the largest planned near-term rocket shrouds is ~30 m. Although we have found a solution for folding a 40 m truss into such a shroud, the unfolding process is substantially more complex than for a 30 m device. We have done dynamical analyses for 80 m trusses, but we have not yet found a good way to package them, nor have we found a good scientific reason for building them, since the angular resolution we once thought needed them can be incorporated onto a 40 m truss.

The interferometers can also be used as two mirror systems, with three possible baselines of 1, 0.714, and 0.286 times the interferometer length. These spacings are useful for measuring the amount of dust in the planetary system, and can also be used for astrophysical studies, which are discussed separately.

The original scheme proposed at the PAR had a large amount of redundancy. For this configuration there is also redundancy. Possible problems are the loss of an outer telescope, or the loss of an inner telescope. In either case it is possible to revert to 2 element nulling, and to use the device as we plan in the SPF concept (selected for NRA study). The larger telescopes, appropriate wavelength region and longer baselines make it possible to study terrestrial planets this way, though with 180° ambiguity of their position, and lowered sensitivity so that all observations take 4 times as long.

Island 4: Tethered Spacecraft Interferometer

The idea for a tethered spacecraft interferometer (TSI) is to use the tethers to off-load the centripetal forces experienced by the collector spacecraft. This option can potentially offer two significant advantages. First, the reliance on propellant to maintain interferometer geometry is significantly reduced relative to the free-flyer, and second, the flexibility of changing the array configuration is still available.

From a structural perspective, a TSI consists of a primary hub, which houses the combiner and the central spacecraft bus, and collector hubs, which are connected to one another by high specific strength cables. The elements in a linear TSI form a daisy chain—the combiner connects to two collectors, which connect to two more, and so on. Each inner collector has two tether canisters, which contain any unreeled tether, the two outer collectors have one canister each, and the combiner hub has four. The additional canisters on the combiner connect it to counter masses, which are used to maintain the system inertia during astrophysical imaging, *i.e.*, they are reeled out/in as the collectors are reeled in/out (Figure 1-6).

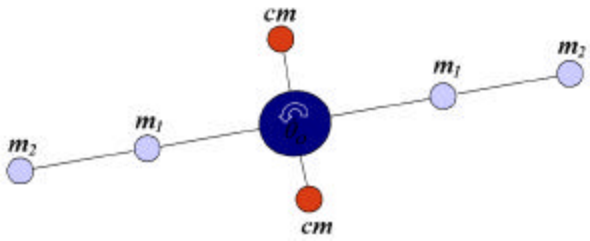

Figure 1-6: Tethered spacecraft interferometer

A structural model of the system is first presented by treating the collector and combiner spacecraft the same as that of the free-flyer system, but with tethers connecting them. However, from a power modeling stand point, this tether system is viewed as a single entity with all the power generated by the combiner spacecraft.

Three spin rate options to fill out the *u-v* plane for general astrophysical imaging are available. The first is to allow the spin rate of the tether system to increase as the collector apertures are reeled in. The second uses counter balances to maintain a constant tether spin rate and the last option uses counter balances to maintain constant linear velocities instead.

Two control issues associated with a tether system were examined: tether pendulum modes and tether vibration rejection. The pendulum modes, which result from the collector spacecraft having a tendency to travel ahead of the tether nominal rotation rate, can be controlled with four different options. As for vibration rejection, an impedance matching control was proposed.

Island 5: Coronagraph

Photon rates

The faintest object that will need to be observed for TPF is a planet at ~ 16 pc. Such an Earth-like planet puts out ~0.005 μJy, or 1.5×10^{-20} W/m^2 between 500 nm and 1 μm. One photon at 760 nm (wavelength of Oxygen A band) gives 2.6×10^{-19} Joules per photon, so 1.5×10^{-20} W/m^2 becomes 0.06 photons/m^2/s. The star gives 4×10^9 times this, or 2.3×10^8 photons/m^2/s. To observe the oxygen A band in the planet, $R = 50$ is needed, or 15 nm, so the fraction of continuum energy in this bandwidth is 0.03 of this, or 0.0018 photons/m^2/s.

The scale collection area

The scale collection area $S = ps^2/4$ is that scale which diffracts at 760 nm into a disk of radius equal to the region where the planet is sought. For a planet at 16 pc, s is approximately 1.5 m, which diffracts to a diameter $?/s$ = 0.1 arcsec, or 0.05 arcsec radius. The planet at 16 pc has a maximum elongation of 0.0625 arcsec, but will typically appear at somewhat shorter elongation.

From the starlight photons, it is possible to determine the phase with an error of 1/v(number of photoelectrons). Then the overall scattered light can be reduced by this factor squared, times the light of the star, *i.e.*, to 1 photoelectron per stability time, per scale collection area.

Each area S contributes 1 scattered starlight photoelectron to the image inside the 0.1 arcsec disk. Thus there are AF/S photons across the disk, where A is the telescope area and F is the fraction available after apodization. However, because the diffraction disk is smaller in area than the 0.1 arcsec disk by a factor S/AF, only a fraction of the photons enter. The two factors cancel, and we find 1 scattered starlight photoelectron in the diffraction disk per stability time.

To achieve this 1 photoelectron, the rms error s associated with the scale S must be sufficiently small that it only diffracts 1 photon into the 0.1 arcsec disk. Let this take a time t. The total number of photoelectrons that could be produced from this patch is 2.3×10^8 m^{-2}s^{-1} $S?t$. Then the scattered light calculation is

$$(?ps/?)^2 = 1 / (2.3\times10^8 \text{ m}^{-2}\text{s}^{-1}\ S?t)$$

For s = 1.5 m and t in seconds,

$$s = 6.0 \text{ pm} / \text{v}(?t).$$

Note that it is essential to make t and $?$ as large as possible to have more planet photons per star photon.

Alternate calculation

Ripples of wavelength 3 m will put their energy into 2 diffraction points 0.05 arcsec from the star image center. The area within the 0.1 arcsec diameter disk is 0.00785 arcsec^2. The area of the diffraction pattern is $?^2/AF$. The number of ripples to fill this area is (1/2) (0.00785 arcsec^2) / ($?^2/AF$) = 0.16AF. These ripples are incoherent, so the rms ripple error associated with the whole is v(0.16AF) of the ripple of any single one. Thus now we are calculating the scattered light from the entire mirror into a single diffraction disk. However, we are allowed to produce 0.16AF times as much light:

$$(?ps/?)^2 = 0.16AF / (2.3\times10^8 \text{ m}^{-2}\text{s}^{-1} AF?t),$$

$$s = 3.2 \text{ pm} / \text{v}(?t).$$

These values define the key achievable parameters for servo control of a coronagraph using the light of the star.

Associated with the coronagraph is also a disturbance spectrum. For a ground-based telescope, it seems reasonable that the disturbance time scale of the atmosphere is shorter than the telescope vibration timescale. For a space telescope, there is a question of whether the vibration amplitude after passive or active damping is sufficient for a coronagraph or not.

For space, the key issue involves spatial wavelengths of 3 m on a structure of 10 m or more in size. The resonant period of the entire structure, if scaled, will increase proportionately with the dimensions. Probably the dominant vibrations will be those with a node in the middle, and the lowest frequency will be that for which the wavelength is double the telescope dimension. Then the amplitude at the shorter wavelength is likely to be smaller than the overall vibration in the ratio of wavelengths squared. Thus, *e.g.*, if the vibration of a 10 m device is 20 nm, the vibration at a 3 m wavelength is likely to be ~450 pm. That is probably around the state of the art. However, if a servo system is used to deliberately damp down mechanical vibrations right through the worrisome frequencies, then one might hope for an order of magnitude improvement before unanticipated new problems surface. But a 45 pm amplitude system has only a modest value of Q:

$$(?ps/?)^2 = 4p^2 (0.045/760)^2,$$

$$= 1 / (7.2\times10^6).$$

$$\text{So } Q \sim 7.2\times10^6 / 4\times10^9 \sim 0.002.$$

This is a rather inefficient system. Let us consider a system operating on starlight. For this system, we can collect 6×10^{-2} m^{-2}s^{-1} $AF?t$ photoelectrons from the planet, and our servo will produce 1 scattered photon from the star in the same period. Therefore the value of Q achievable is 6×10^{-2} $AF?t$. The best this can be is 1, and so provided $AF?t > 20$ m^2, this is possible. Now with $t \sim 0.03$ s, apodizing factor $F = 0.5$, and $? = 0.14$, we find $A > 9500$ m^2. This is a 110 m telescope, and seems implausible for space. As we shrink the telescope, Q decreases linearly with the area: for a 950 m^2 telescope we arrive at $Q = 0.1$; for a 95 m^2 telescope $Q = 0.01$; and for a 13 m^2 telescope $Q = 0.002$. Thus for such a small telescope, no improvement over a mechanical system seems helpful.

Performance in Space

We need to observe a planet with SNR = 25 and $R = 50$ to detect the oxygen A band. In the $R = 50$ band, we get 0.001 photon/m^2/s *F?*, or 7×10^{-5} counts/m^2/s at efficiency 0.07. To make an observation with SNR = 25 we need 625 counts (in the absence of background). This will take $[(8.9\times10^6\ \text{m}^2)/A]$ seconds.

For $Q < 1$, the time must be increased by a factor $1/Q$ to $[(8.9\times10^6\ \text{m}^2)/AQ]$ seconds. So if we allow 10^6 seconds for the observation, we find $AQ = 8.9$ m^2. Then ~222 m^2 (16.8 m telescope) should make the observation, with $Q = 0.04$. If we increase the observing time to 5×10^6 seconds, then the area needed is 100 m^2, equivalent to an 11.3 m telescope.

Performance on the Ground

It is possible to directly relate telescopes on the ground to telescopes in space, because the only critical factor is the stability time, which is 30 times longer in space than on the ground. We find then that the telescope area on the ground must be increased by a factor v30 or the radius increased 2.34 times, and thus the telescope sizes for 10^6 seconds and 5×10^6 seconds from the ground are 39 m and 26 m. Because of more limited night time from the ground and weather, it would seem that the larger size is appropriate, but one could stretch a ~30 m telescope to extremely long integrations where a source deserved it.

Architecture Evaluation

The KTA approach described in Section 5.1.1.1 was implemented by the Lockheed Martin Team in the evaluation of the five selected TPF architecture "Islands" (options). Key members of the team (LMSSC, UA & MIT) convened at a one week meeting at LMSSC-Sunnyvale during November 2000 to accomplish the final evaluation process. Evaluation criteria were reviewed just prior to the evaluation assuring common understanding by all team members. These criteria were defined as follows:

Risk is the danger that the concept will encounter a major technological hurdle that prevents it being implemented in cost and time.

Reliability/Robustness is the mean time to failure/the amount of redundancy placed in a system without change in performance with a failure

Heritage (Legacy) is the ability to make technological and experiential progress towards Life Finder and Terrestrial Planet Imager (TPI)

Astrophysics Opportunities is the assessment of general astrophysics that can be performed.

Planetary Detection consists of the science requirements contained in Exhibit 2 of the TPF study contract.

Technology Requirements considers the degree of technology development required for the various architectural options.

Life Cycle Cost (LCC) is based on the team assessment of the cost of each of the architecture options for all program phases (BCDE). Program schedule spans were estimated for each architecture to support LCC estimating.

A review of each of the technical features of candidate architectures was accomplished. The evaluation process was held in round table fashion with all key team members participating.

Criteria weighting was discussed and following consensus relative numbers were assigned to each criteria. The team then evaluated each architecture option and developed a relative score indicating how well the option met the criteria in comparison to all other architecture options. The product of the relative score and the assigned weighting of the criterion provided the score for the option with respect to that evaluation criterion. For example, Island 3 scored highest in technology requirements criteria (indicating the least amount of technology development compared to all other architecture options) so it was scored a 10. The weighted score was determined as the product of the relative score and the criteria weighting of 9, which yielded a score of 90. The evaluation process continued through completion (all architecture options assessed against all criteria) and a total score was determined by summing the individual criteria scores for each architecture. The results of the evaluation are shown in Table 1-4.

Table 1-4: Architecture study trade results

Configuration Number	Number of Telescopes	Architecture	Planetary Detection	Astrophysics Opportunities	Technology Requirements	Risk	LCC Phase B C, D	Reliability/ Robustness	Heritage Legacy	Total
		Weighting	10	5	9	8	10	7	4	
Island 1	3 Collectors 2 Combiner/ Collectors	Separate S/C Interferometer (SSI)	10 (100)	5 (25)	9 (81)	9 (72)	10 (100)	10 (70)	10 (40)	488
Island 2	1	Segmented Mirror Interferometer (SMI)	10 (100)	5 (25)	7 (63)	7 (56)	4 (40)	5 (35)	5 (20)	339
Island 3	4 Collectors 1 Combiner	Structurally Connected Interferometer (SCI)	10 (100)	5 (25)	10 (90)	10 (80)	8 (80)	7 (49)	8 (32)	456
Island 4	3 Collectors 2 Combiner/ Collectors	Tethered S/C Interferometer (TSI)	10 (100)	5 (25)	6 (54)	6 (48)	5 (50)	3 (21)	6 (24)	322
Island 5	1	Coronagraph	10 (100)	5 (25)	3 (27)	2 (16)	3 (30)	2 (14)	4 (16)	228

The leading architecture to meet Exhibit 2 requirements is the free-flyer (SSI, Island 1). This is essentially the same system as the TPF monograph. The structurally connected interferometer (SCI, Island 3) has the least development, however costs increase as the interferometer baseline increases. The coronagraph, Island 5, has difficulty because of low photon rates for the objects we are observing. Islands 2 and 4 have potential.

Exploration of Concepts

For the exploration of concepts phase, we first developed a plan to compare devices:

1. All devices must satisfy the TPF requirements of numbers of stars to be observed, SNR of habitability determination and SNR of Biomarker(s).
2. Quality of information about the terrestrial planet (spectral region, spectral resolution and signal/noise limit) is compared.
3. New technology needed, especially development time, cost, and assessed risks are compared.
4. Weight, size, packaging, and deployments are compared.
5. Relative benefits, costs, *etc.* are weighted and summed to give a single metric.

One starting point was to consider devices with refractive elements. The problems with these are first that they are liable to impose the spectral signature of the material on the planet. Calibration while possible would be an annoyance, and might well impose features just where there was a great scientific interest.

Another was to consider the possible spectral regions where the appropriate information might be obtained. Surprisingly, the mm-wave region looked extremely interesting for this, but the technical demands were so high that this region was rapidly discarded. We then found interest focussed on two spectral regions, the mid-IR and the visible, both of which would provide interesting scientific information. We preferred to start with the infrared, because it gave us information about the planet size and temperature not usually available from the visible, but felt that detection in the visible was sufficiently interesting to deserve exploration.

The angular resolution and contrast were major features for the selection process. If the achieved contrast with the planet is reduced as a result of additional signal from the star, dust, *etc.*, the observing time is increased by the ratio of the measured signal for the planet position divided by the signal due to the planet alone. For the interferometric infrared TPFs, the main signal for the bulk of the stars is that due to local zodiacal dust. Typically this signal is 10^{-4} to 10^{-5} of the star, and so is some 100 to 1000 times larger than the planet signal. However, the planet produces some 20 times as many photons as in the visible, so that the signal to noise ratio for an observation of a certain duration would be similar for observing in the infrared with the background, than in the visible with zero background. The difference is that the star signal only needed suppression in the IR by a factor of about 10^5, whereas to get similar performance from the same area of optics in the visible required a suppression of a factor 4×10^9.

It was this large factor that eliminated external occulting masks for the visible from our consideration. Fresnel diffraction control to that level seemed to require a very large occulting mask with very precise control. It also excluded the concept of Fresnel lenses, which have been developed at Livermore.

After these types of devices had been rejected, we found that we were then thinking in terms of various types of interferometer for the infrared, and coronagraphs for the visible. We rejected the possibility of infrared coronagraphs rapidly. Suppose for example that we were required to make an infrared coronagraph so that it produced an angular resolution of 0.05 arcsec at 17 μm. Even an ordinary telescope to produce that resolution would require a diameter of *?* = *?*/*D*, or 68 m. To get a coronagraph would likely require at least twice that diameter, and it seemed unlikely that optics of 130 m width and 130 m to the focus could be competitive in weight, size, packaging, and deployment.

So we were reduced to a relatively straightforward comparison of ways of achieving a coronagraph in the visible and an interferometer in the infrared.

System Trades

The MIT team members developed a process and a software tool, based on a quantitative systems engineering methodology, to conduct trade studies for comparison of competing system architectures for TPF. The TPF mission analysis software (TMAS) package is a comprehensive, modular, expandable, and robust tool for trading TPF mission architectures using unified and quantitative metrics. TMAS consists of 6 macro-modules that model the physics and processes that distinguish between competing system architectures, including structurally connected (truss)

and separated spacecraft (formation flying) concepts. Ultimately, each design is evaluated by a performance assessment module (GINA), which computes the capability, performance, and cost of each architecture. The cost per image metric is the primary metric used to trade architectures against each other. This metric represents the ratio of the total lifecycle cost of the mission divided by the number of useful "images" returned, where "images" represent the total number of surveys and spectroscopic observations accomplished during the mission lifetime. Limited resources, in the form of personnel and time, determined the level of fidelity incorporated into the model. The team focused on developing models for the processes with the greatest likelihood to contribute to the differentiation between architectures. After using benchmark spacecraft configurations, previously developed by industry teams, to validate the TMAS package, the team conducted one dimensional trade studies from a baseline spacecraft configuration to evaluate general trends.

5.1.1.3 Recommendations

Science

There are several unresolved science issues that could impact the primary goal of TPF to detect and characterize planetary systems. These include:

?? Major role of giant planets in setting up the volatiles and collisional status of terrestrial planets.

?? Frequency of giant planets with large orbits as in the solar system.

?? Frequency of old planetary systems with planets in close orbits like Jupiter and Saturn. These are not expected to be stable unless the orbits are circular.

Significant progress in the answers to these questions could be made with precursor missions. Characteristics of such precursor missions are as follows:

?? Should be able to see and characterize for habitability any very close by terrestrial planets.

?? Spectral region should be in the spectral region needed for a full-scale TPF mission to support validation of the technology (*i.e.*, the precursor needs to be a nulling IR interferometer).

We consider main sequence and subgiant stars of types F-K, with predicted planet separations exceeding 0.1 arcsec, and with the star closer than 15 pc. These are the stars that could be examined with a 21 m truss system. After removal of binaries there is a 39 star list. It includes 20 F stars, 12 G stars and 7 K stars. Similarly one can see that by increasing the optics size and truss length by a factor 1.33, the number of stars is expected to increase by a factor 2.37 from 39 to 92, and in fact 91 stars are found. So the cube law seems to work quite well. According to this, the system to observe 100 stars would need a 30 m truss, and the system to observe 150 stars would need a 34 m truss of the type we consider. The numbers are also somewhat adjustable because one can include more F stars, and find resolvable earth-like planets at somewhat larger distances from the sun, or look for stars where the predicted planet separation is somewhat smaller. If in contrast we were to look for a minimal TPF, and were to go towards even smaller trusses and optics, we find that a system to observe 10 stars would need a 14 m truss. Correction for low galactic latitude is expected to be about 10%.

Astrophysics opportunities presented problems for every concept considered. Free flying systems required an additional mission to fill in short baseline information. Fixed baseline systems were

unable to supply the long baseline information. In all cases, optimization for planet studies de-optimized astrophysical abilities and vice versa.

Precursor Mission

During the Phase 1 study it was determined that it was prudent to develop the full-scale TPF system in an incremental manner to reduce technology risk, minimize the schedule, reduce cost and obtain valuable science data in a more timely manner. The Lockheed Martin Team recommends inclusion of a TPF Precursor Mission with the principal objectives as follows:

?? Determine frequency expected for terrestrial planets prior to commencement of full-scale TPF program to reduce cost.

?? Determine technological barriers and unknown barriers associated with the nature of planetary systems to reduce risk/cost of a follow-on full-scale TPF mission.

?? Demonstrate science capabilities and technology of a nulling IR interferometer operating in space.

?? Provide a relatively low cost, accelerated program for planet detection and characterization.

The approach started by documenting the components of a mission, and discovering where costs could be lowered. Thus a launch rocket is necessary regardless of mission, and it must take the device into an environment where the passive cooling concept can be tested. This eliminates small rockets, and essentially moves one to consider Delta II or larger rockets and fall away orbits (SIRTF-like). Also the interferometer must be passively cooled, and there must be a cryogen-cooled beam-combiner/detector package, and telescopes.

A cost analysis conducted by the team as part of the evaluation process suggests that for minimal systems a free flyer (separate spacecraft interferometer) is more expensive than other options. This eliminated Islands 1, 2 and 4. Island 5 (coronagraph) was considered as having a high technology development compared to a nulling IR interferometer so was eliminated as a solution for a precursor mission. The resulting option is the structurally connected interferometer (Island 3).

We have considered two potential precursor missions, shown in Figure 1-7. The first of these is a device for looking at young warm Jupiter-like planets, which are self-luminous at 5 µm because of a window in the planet atmosphere opacity. It addresses two of the three unresolved science issues identified in the previous section. The concept uses two 60 cm mirrors separated by 9 m, as a nuller. The beam combiner is in a solid hydrogen cooled dewar. The truss has appropriate exterior surfaces to provide the first stage sunshade. This device has been submitted for the Extra-Solar Planets Advanced Mission Concepts NRA, and has been accepted for further analysis.

As compared with this slimmed down concept, a device for observing terrestrial planets needs a larger rocket shroud to handle a larger truss, better passive cooling, a three stage nuller (though using the same processes at the same precision as above), four sets of telescope optics as compared to two, and the primary mirrors need to be larger, at least 85 cm diameter. More sensitive devices can be made with larger mirrors and longer trusses all the way up to fulfilling a complete TPF mission. The angular resolution of a 21 m truss system at 10 µm would be adequate for looking at any planet no less than 0.1 arcsec away from its star at maximum elongation. Some planets closer to their star could also be seen—the absolute cut off is wavelength dependent, and TPF will seek planets in a wavelength range.

The 21 m system would be folded in four segments of equal length for stowage in the Delta II payload fairing. The spacecraft would be placed either in an Earth-trailing or L2 orbit to achieve sun shielded optical system temperatures of 25 K–30 K. The team determined that the precursor program could result in a launch in the 2007 timeframe at a cost less than 1/4 of the full-scale TPF program.

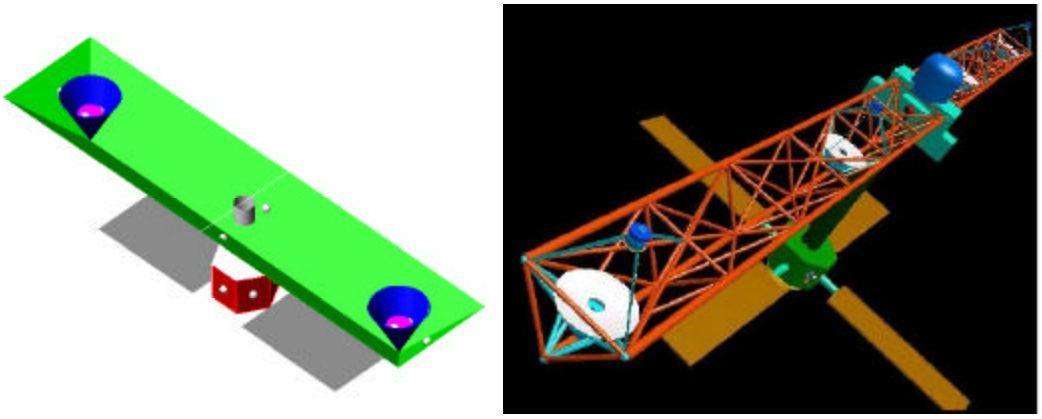

Figure 1-7: Precursor concepts: 9 m (left) and 21 m (right)

Cost

Life cycle cost estimates during Phase 1 were derived using the GINA program and estimates by team members. Costs were estimated for each of the five architectures (Islands) and two versions of a precursor. Cost ranges were developed and applied to the various architectures as shown in Table 1-5. Island 1 (separate spacecraft interferometer) was determined to be the least expensive TPF system at a cost of $1.75–$2.5 billion. The Island 3 Precursor (21 m structurally connected interferometer) was determined to be the least expensive system with a cost of $0.3–$1.0 Billion.

Table 1-5: Life Cycle Cost Estimates

Costs include development, phase A/B/C/D, and LV		
Cost categories		
Very high	> $2.5 billion	
High	$1.75–$2.5 billion	
Moderate	$1.0–$1.75 billion	
Low	$0.3–$1.0 billion	
Cost Assessment		
Island 1	Separate Spacecraft Interferometer	High
Island 2	Segmented Mirror Interferometer	Very High
Island 3	Structurally Connected Interferometer	Very High
Island 4	Tethered Spacecraft Interferometer	Very High
Island 5	Coronagraph	Very High
Island 1	Precursor	Moderate
Island 3	Precursor	Low

Part 2: Phase 2 Final Report for

TPF Pre-Formulation Phase Study

29 March 2002

In response to:

Terrestrial Planet Finder Contract 1217283
Jet Propulsion Laboratory
4800 Oak Grove Drive
Pasadena, CA 91109

Submitted by:

Lockheed Martin Space Systems Company
Missiles & Space Operations
1111 Lockheed Martin Way
Sunnyvale, CA 94089

Table of Contents

5.1.1.1 Lockheed Martin Architecture

Mission Summary

The Lockheed Martin Team (LMT) was assigned by JPL following the PAR presentation to conduct Phase 2 studies of two architectures: the Structurally Connected Interferometer and the Separate Spacecraft Interferometer (Free Flyers), both using Nulling IR Interferometer technology. We refined the TPF science requirements and optical system concept, updated computer models, derived system and subsystem requirements, performed system trades and analyses, defined internal and external interfaces, determined technology requirements and status, defined programatics and prepared cost estimates for Phases BCDE. The results of these efforts were presented at the Final Architecture Review held in December 2001.

We evaluated configurations with a range of baselines. The on-orbit configurations are sketched in Figure 2-1. Table 2-1 shows the optics and overall science capability for the specific baseline instruments studied, and gives estimates of the Phase BCDE cost in Y2002 dollars. Detailed science requirements and capabilities that can be achieved with these configurations are listed in the table 2-2. This report describes results for the 40 m configuration that meets all of the TPF science requirements, while the adjustable baseline free flyer configuration will also support astrophysics science.

Our goal for Phase 2 was to develop a cost-effective, science responsive TPF program. Implementation of the phased incremental development approach provides for early demonstration and validation of relevant technology while yielding important science data for planetary detection and characterization. In particular, IR nulling technology development and validation must be completed for the TPF program to be successful. We are proceeding with testbeds to support development of the beam combiner. The technology readiness levels of the various aspects of the nulling interferometer TPF are summarized in Table 2-3.

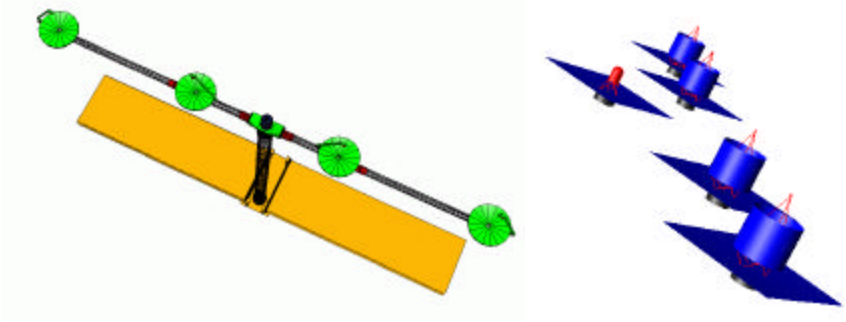

Figure 2-1. 40 m baseline structurally connected and free flyer TPF configurations

Table 2-1. TPF configuration summary

Mission	Interferometer Baseline	Wavelength	Telescopes			Science Capability	Cost*
			Number	Aperture	Temperature		
Precursor	9–18 m	7.5–12.5 μm	2	0.6–1.4m	40 K–60 K	Jupiters (13pc)？ Earths (12 pc), O_3	$293M–$390M
Reference	21–40 m	7–17μm	4	1.7–3.5 m	30 K–45 K	Earths (12 pc), H_2O, O_3, CO_2 (8 pc), ？ Earths (22 pc), H_2O, O_3, CO_2 (16 pc)	$843 M–$1,731M
Future	Variable (FF)	3–23μm	4	3.5–6.0 m	30 K–45 K	NASA Planetary Detection Rqmts + astrophysics	~$2,500 M

*Cost estimates include 30% contingency.

Table 2-2. Comparison of NASA TPF requirements and LM architecture capability						
General Mission Assumptions		NASA Rqmts	LM TPF Configuration Capability			
			40 m	21 m	18 m	FF
1	Sky coverage	60%	>90%	>90%	>90%	>90%
2	Mission duration (years)	5	5	5	4	10
3	Nominal planet is defined as a solid body with Earth radius at 1 AU, T=270 K (Jupiters for 9 m B/L)					
4	The planet detection and characterization program will be allocated ~50% of the design mission lifetime with the remainder of the lifetime allocated for general imaging and spectroscopy.					
5	Spacecraft use non-nuclear power sources.					
Planet detection and characterization						
1	Number of stars (F5-K5) surveyed for planets (R=3, SNR=5)	150	348	44	30	500
2	Number of scans for CO_2/H_20 (R=20, SNR=10)	30	>100	18		>100
3	Number of scans for Ozone/strong CH_4 (R=20, SNR=25)	5	>25	5		>25
4	Spectral band (mm) (Zodiacal light limited)	7–17	7-17	7-17	7.5-12.5	3-23
5	Spectral resolution	20	20	20	20	100
6	Maximum distance of ozone detection (pc)	10	>20	13	6	>20
7	Minimum distance of planet detection (pc)	3	3-22	3	3	22
8	Exo-zodiacal dust will be the same as in our own solar system for requirement, up to 10 times the solar system level.					
9	Follow-up (high spectral resolution) surveys are uniformly distributed throughout the volume of the initial survey.					
10	Point source sensitivity: 5 ?, 2 hr at 12 μm, R=3. (μJy)	0.3	0.13	0.53		
High resolution imaging (TBR)						
1	Imaged objects for 5 year mission	800				1600
2	Resolution at 3 μm (milliarcsecond)	0.75				0.75
3	Band (μm)	3-17				2-40
4	Spectral resolution	3-300				3-300
5	Special purpose spectral resolution (FTS mode) in specified lines					
7	Effective minimum baseline for synthetic imaging (m)	100				<50
8	Dynamic range in reconstructed image	50:1				100:1

Table 2-3. Technology readiness levels for nulling IR interferometer TPF				
Configuration	40 m SCI	21 m SCI	9 m SCI	SSI (FF)
Telescopes	6 (NGST)	7	8/9	6 (NGST)
Beam combiner	4	4	4	4
Detector cooling	8	8	8	8
Spacecraft	9	9	9	
Electrical power	9	9	9	9
Guidance & control	9	9	9	
Software	5	5	5	
Vibration control	6	6	7	
Truss structure (w/o precision deployment)	8	8	9	N/A
Sunshield	5 (NGST)	5 (NGST)	7	5 (NGST)
Contamination control	9	9	9	9
Integration & test (based on facilities availability)	9 (seg tests)	9	9	
Orbit	6 (SIRTF)	6 (SIRTF)	6 (SIRTF)	
Launch vehicle	9 (pkg TBR)	9	9	9
Ground system	7 (SIRTF)	7 (SIRTF)	7 (SIRTF)	7 (SIRTF)

Optics

The fundamental optics design that we have considered is scalable to accommodate a range of telescope baseline and aperture requirements. It also does not depend on the number of collectors, so that it may directly adapted to/from a two collector test lab or precursor mission. A

schematics of our optics design concept is shown in Figure 2-2. For the specific configurations described in this report, the optics system requirements are listed in Table 2-4.

Table 2-4. Optics System Requirements

Baseline	9 m	21 m	40 m	Free flyer
Wavelength Band (TBR)	4–12 μm	7–17μm	7–17μm	3–23μm
Null depth	1.0E-04	3.7E-05	3.7E-05	3.7E-05
Telescope Diameter	0.6 m	1.7 m	3.5 m	6 m
f-ratio	*f*/1	*f*/1	*f*/1	*f*/1
Telescope Temperature	60 K	40–45 K	40–45 K	40–45 K
Optical Path Errors	7.2 nm	10.6 nm	10.6 nm	10.6 nm
Transmission Asymmetries	0. 7%	0.4%	0.4%	0.4%
Pointing Jitter	82 mas	54 mas	26 mas	15 mas
Diff'l Polarization Rotation	0.4°	0.2°	0.2°	0.2°
Diff'l Polarization Delay	0.8°	0.5°	0.5°	0.5°

Collectors

Each telescope is a Cassegrain *f*/1 with flat tertiary on 2-axis flex pivots. The short focal ratio allows the telescope to be conveniently packaged in the launch vehicle shroud. The quality of the optics is diffraction limited at 2 μm for phase detection and correction. Cold baffled tubes link the collectors to the beam combiner.

The technology for collector mirrors 1.7 m and smaller will either be cryo-null figured beryllium, as used in IRAS and SIRTF, or glass. The technology for the larger collector mirrors (3.5 m, 6 m) will be derived from NGST technology.

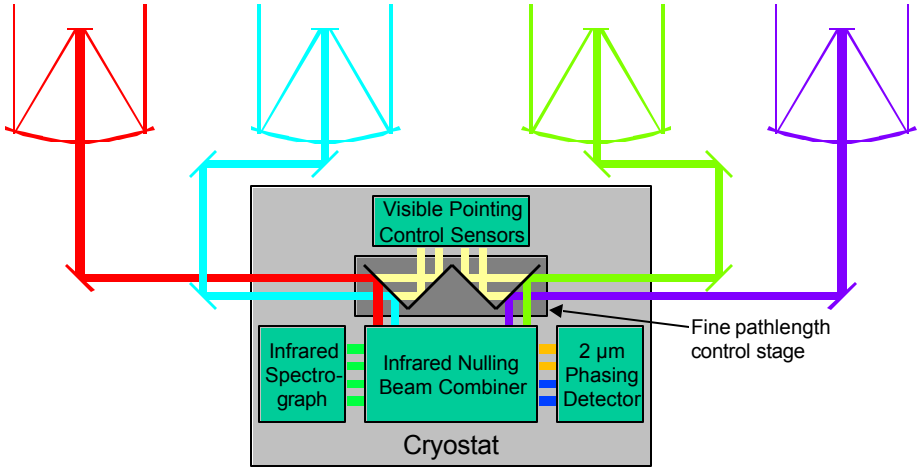

Figure 2-2. TPF optics schematic

Combiner

The nulling beam combiner (NBC) is an amplitude balanced imaging interferometer, based on a modified Mach-Zender (MMZ) concept published by Serabyn & Colavita (Applied Optics, Vol. 40, 1 April 2001, pp. 1668-1671), shown in Figure 2-3. The Serabyn & Colavita concept provides a fully symmetric nulling interferometer by introducing the field flip using a pair of periscope mirrors prior to beam combination. We consider a variation of this design, using dielectric phase plates to introduce the p phase shift rather than the right-angle periscopes. This modification breaks the symmetry of the Serabyn-Colavita nulling beam combiner, but it allows us to use the unbalanced ("bright") outputs to provide phase control information at a shorter wavelength

(~2 μm), where the phase plate produces ~3p/4 phase shift. In this way, the phase is measured on the identical optical path that produces the science data.

A 2 μm detector with a 200 Hz readout produces a 20 Hz authoritative control bandwidth to the path length correction. Fine path length adjustment is supplied by mounting the entrance dichroic mirrors and the pointing sensor mirrors on a stage that moves by PZTs along the axis of the incoming beams, as shown in Figure 2-2.

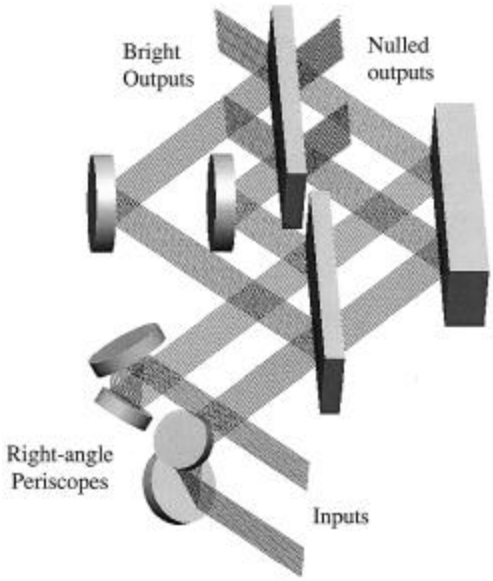

Figure 2-3. Serabyn & Colavita modified Mach-Zender beam combiner

The entrance mirrors to the NBC are gold film, so that IR light is reflected and visible light is transmitted. The visible light from each collector is directed onto a quad cell, which tracks pointing displacements and corrects for them by controlling the tertiary steering mirror on the collector.

The output of the NBC is fed into a prism spectrograph, with resolution $R \sim 20$. The required spectrograph temperature is 17 K. The detectors are SIRTF heritage Si:As BIBs, cooled to 8 K. A chopper placed in front of the detectors allows for suppression of low frequency background noise.

The nulling beam combiner, visible light pointing sensor, phase detector, and spectrograph are all mounted on a single optical bench inside the cryostat. The optics are mounted and aligned on the optical bench warm. The assembled optical bench is then tested at flight temperature, and the alignment is verified and corrected as needed. The verified optical bench is integrated into the cryostat, and the alignment is re-verified with the cryostat in flight configuration and at flight temperature. From this point, the integrated cryostat is never warmed up again, so that the only environmental change the optics see is the launch environment. This method requires a window transparent in the range 0.5 μm to 20 μm, which could be retained or removed in flight, depending on how the cost/performance trade works out. The significant advantage of this approach is the ability to verify key optics and alignment requirements by test in the flight configuration with minimal reliance on analysis.

A schematic of our combiner system is shown in Figure 2-4. Each pair of collector inputs utilizes the same MMZ NBC. The outputs of each pair of combined beams are fed backwards into the

same MMZ again, this time without a p phase shift. Because the same MMZ optics are used for all four beam combinations, the design can be readily adapted for a two-collector system. Conversely, a simplified two-collector combiner testbed of this type will serve to demonstrate all of the key technologies necessary for the four-collector combiner.

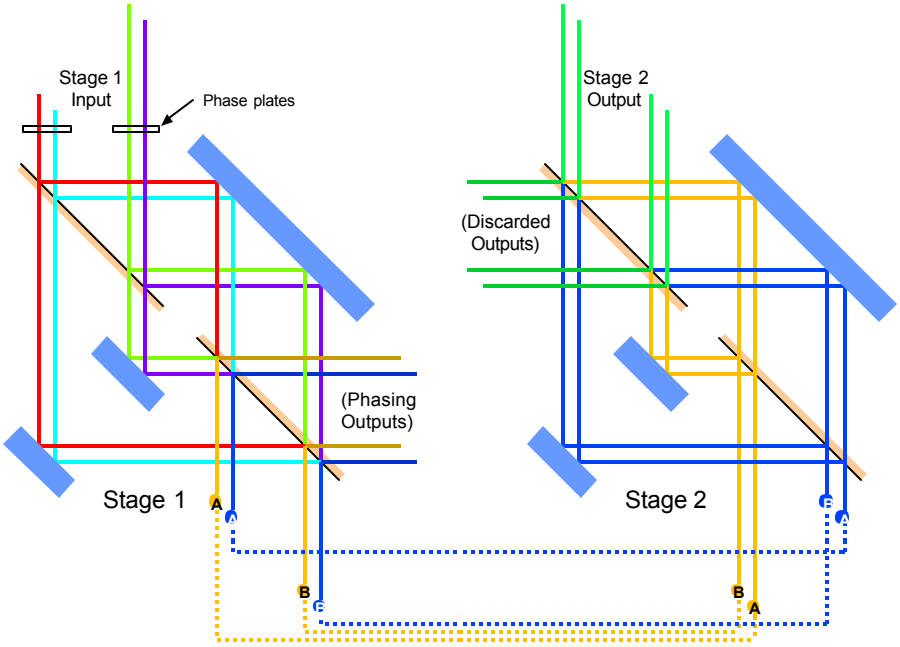

Figure 2-4. TPF optics design

Figure 2-5 shows our infrared nulling technology roadmap, including the technologies needed and the phasing of the testbeds, to support a precursor launch in the 2007 timeframe, and a full TPF launch in the 2015 timeframe.

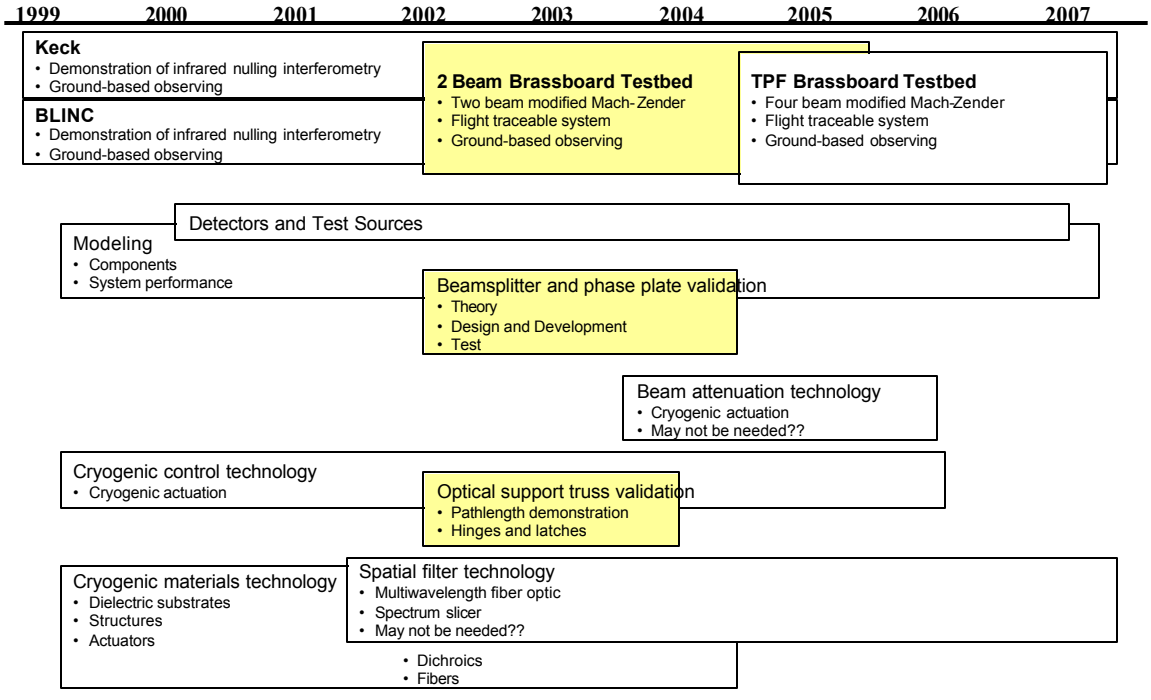

Figure 2-5. Infrared nulling technology development and validation roadmap

Detectors

Three types of detector are required for the TPF truss interferometers, 7 µm–18 µm wavelength for data, 0.5 µm–0.9 µm for star position, and 2 µm for phase detection.

Data Collection

The detectors required for collecting data will integrate for a period of ~8 seconds to 1 minute, and then be read out. The characteristics of SIRTF detectors as used in IRAC appear appropriate. These are 256x256 Si:As detectors supplied by SBRC (now Raytheon). The DQE at 8 µm is 70%, read noise is 10.8 e- (Fowler 32 sampling), and dark current is 3.8 e-/s.

The TPF Book assumes DQE folded with optics into an overall efficiency term of 4%, read noise 1 e-, dark current 5 e-/s. This read noise is clearly optimistic, relative to SIRTF, and we ask whether this will cause any problems if we use detectors whose performance is identical to SIRTF.

The local zodiacal background puts 2900 photons/second into R=0.2 and a 10 micron diffraction patch, regardless of telescope size, and with allowance for likely inefficiency. Thus if R=20, adequate for detection of ozone, there will be 290 photons per second detected. We can assume that this radiation is split between six detector pixels, and so is 48 counts per second per detector. Over 8 seconds (a likely shortest integration time), the signal count is 384, the dark count is 30, and the read noise is 10.8. Thus the overall noise will be +/-23 counts, whereas from signal alone it would be 19.6, an increase of 17%. This would result in an increase in integration time of 37%. This is just acceptable. If the integration times were extended to 60 seconds, the noise would be 57.4 whereas from signal alone 53.7 is expected, an increase of 7%, and an increase in observing time of 14.5% which is certainly acceptable. We conclude that SIRTF detectors are therefore adequate, but note however that there is a need to keep the number of illuminated pixels in the spectrograph focal plane to a minimum.

Star Position

These detectors are assumed to be CCDs. The temperature of the external shell of the dewar is 40 K–60 K, and we would certainly expect CCDs to operate at these temperatures. However, we are expecting the beam combiner itself to be at about 17 K, and at this temperature there may need to be a selection of CCDs to find ones where the current is not frozen out. Alternative detectors do exist, but we are concerned to take advantage of the small size of pixels, and determine star positions to photon limited precision, and CCDs would seem to be best for this. Verification of appropriate CCD performance is needed.

Phase Detection

2 µm detector arrays are being used at LN_2 temperatures in the BLINC mid-IR beam combiner, and with these, too, verification of appropriate performance at somewhat colder temperatures is required.

Structurally Connected Configurations

Our 40 m baseline configuration, shown in Figure 2-1, consists of four collector telescopes and a cryostat mounted on a truss. The truss is mounted on one end of a boom by means of a two-axis rotation mechanism, and the spacecraft bus and sunshield are mounted on the other end. The

boom is aligned with the spacecraft-sun vector so that the sunshield can shade the cold components. The truss is rotated by a pitch actuator to any angle from perpendicular to parallel to the boom. With 360? rotation of the entire observatory about the boom centerline, the telescope line of sight can be placed anywhere within 90? of the anti sun line, to give full 2? instantaneous sky coverage. A yaw actuator rotates the telescope truss about the telescope line of sight to provide the necessary angular sweep of the target star.

A detailed finite element model of the 40 m baseline TPF configuration was constructed to evaluate on-orbit vibration characteristics. The model consists of 41063 nodes and 68424 elements. Because the mechanical design is evolving, conservative assumptions were used specify the stiffness characteristics and other design parameters. NASTRAN was used to evaluate the vibration modes to 100 Hz. Figure 2-6 shows the first vibration mode at 0.53 Hz and the modal density.

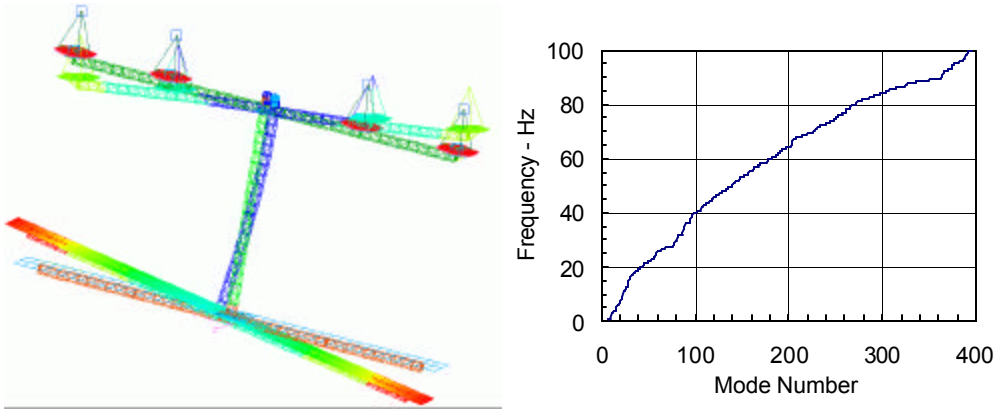

Figure 2-6. First vibration mode and modal density.

The 40 meter TPF with the SIRTF spacecraft bus and adapter is stowed in the Delta 4 EELV 5 m diameter fairing, as shown in Figure 2-7. The clearance between the stowed mirror truss and the fairing is 30 mm. The stowed frequency is greater than 11 Hz. The sunshields are deployed first using two bistems to unroll the shields from the drums used for stowage. The TPF vertical mast is then deployed using a space qualified Able ADAM mast. The mirror support truss is then rotated into position and locked. Finally the secondary mirrors of the 3.5 meter collectors are deployed.

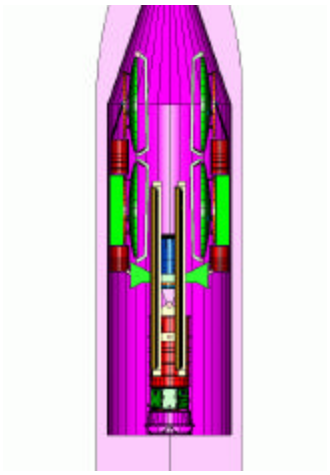

Figure 2-7. 40 m TPF in launch configuration.

Pointing, Path-Length Control and Vibration Mitigation

Control and operational requirements for structurally connected interferometers with baselines up to 40 meters (Table 2-5) can be achieved using a conventional spacecraft attitude control system, active pointing and path-length control, and a vibration mitigation approach that does not rely on structural damping.

Table 2-5. Top-level performance and operational requirements

Baseline	40 m	21 m	9 m
Null depth	3.7E-5	3.7E-5	1E-4
Pointing jitter	26 mas	54 mas	82 mas
Optical path length error	10.6 nm	10.6 nm	7.2 nm
Slewing (goal)	60? in < 1 hr	60? in < 30 min	
Baseline rotation about line of sight	8 hrs/rev (goal: 2 hrs/rev)		

The precision structure supporting the collectors and beam combiner operates at cryogenic temperatures where structural damping can be very low and difficult to predict. The proposed approach to mitigate risks associated with mechanical vibrations consists of: Demonstrating a system level solution that does not rely on structural damping, which is provided by passive electromagnetic tuned-mass dampers (TMDs), reducing disturbances at the sources, e.g. reaction wheels, and using active compensation to reduce jitter and path-length-errors.

Control System

The basic attitude control system for TPF is based on SIRTF, main components such as reaction wheels, wheel isolation, star trackers, and gyros are commercially available and have been demonstrated in flight. Fine pointing control is achieved through active jitter compensation using detector signals and fast steering mirrors. Optical path-length control is implemented using fringe tracking and active delay line.

Slew, baseline rotation and momentum dumping were used to assess system capabilities and size the reaction wheel assembly (RWA). The results show that existing wheels can be used to meet the required performance for all configurations considered, 9, 21, and 40-meter baseline. The goal of 60-degree slew in 30 minutes or less for the 9 and 21-m configurations is easily achieved. While the 60-degree slew times for 40 and 80-m configurations are 1.3 and 3.2 hours respectively. Time to spin-up to 1 revolution in 8 hours is under 10 minutes for all configurations. The frequency of momentum dumping is about once every 10 days for the 9 and 21- meter baselines, and once a day for the 40-meter baseline.

Performance Analysis

A dynamic model of TPF was generated that includes: Rigid and flexible body dynamics, detailed model of the ACS and fine pointing sensors and actuators, simplified model for computation of path-length error, and detailed model of the control system including a dual mode Kalman filter and attitude control logic. Frequency analysis was used to assess the effect of reaction wheel disturbances on performance, measured as pointing stability and path-length error. A high-fidelity simulation including all known error sources was used to assess on-orbit performance. All modes up to 100 Hz were included in the analysis. For the 40-m configuration, this means 271 modes with the first mode at 0.22 Hz. Structural damping of 0.1% was assumed for all modes, justified by the approach of using TMDs to provide system level damping.

Results show pointing control within requirements and significant performance margin for all configurations. For the 9, 21 and 40-m configurations, path-length errors were also within requirements, except for wheel speeds below about 300 rpm. This can be resolved by operating the wheels at speeds larger than 300 rpm with minimum impact in overall system performance. For the 80-m configuration, where larger wheels are used to achieve adequate slew and spin-up times and momentum storage, the path-length errors exceeded the requirement for a few wheel speeds between 600 and 2100 rpm. Quieter wheels or specially balanced wheels should be used to reduce these errors. Frequency analysis results are shown in Figure 2-8 for the 40-m baseline.

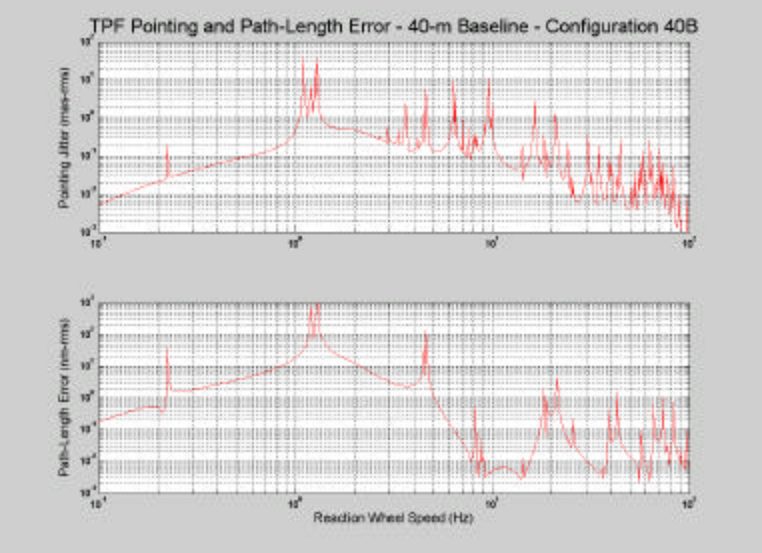

Figure 2-8. Pointing and path-length errors due to RWA disturbances– 40-m baseline

Results of high-fidelity time domain simulations are summarized in Table 2-6 for the system operating in science mode and wheel speed near its mid-range (~3,000 rpm). These results include all error sources, *e.g.* wheel disturbances and sensor and actuator noise, non-linearities and quantization effects, and therefore represent a preliminary on-orbit performance estimate.

Table 2-6. Performance predictions from high-fidelity simulation

Baseline	40 m	9 m
Pointing Jitter (mas-rms)	0.7	2.7
Optical Path-Length Error (nm-rms)	0.9	1.2
All error sources included		

These results show that requirements on pointing stability and path-length error can be achieved with adequate margins for systems with baselines from 9 to 40 meters. Therefore, for a structurally connected space interferometer, a relatively mature system and control architecture can achieve the pointing and control requirements for the TPF mission.

Risk Assessment

The basic spacecraft ACS is mature and flight proven presenting low risk. The use of tuned mass dampers to achieve system level damping has been demonstrated in simulation and requires hardware demonstration at the proper environment. The risk associated with this approach and technology is considered low to moderate. Pointing jitter control using detector signals in a feedback loop to drive a fast steering mirror is a mature concept, but operation and performance at cryogenic temperatures should be demonstrated. The risk associated with this technology is

considered low. Active path-length control using feedback signals from a fringe tracking system and an active delay line is the control system technology requiring most development. This is due to the unique approach for phase detection, which has been demonstrated in a ground telescope, but needs to be demonstrated in an active closed-loop system, followed by demonstration in the proper environment. The risk associated with this technology is considered moderate.

Free Flyer Configurations

Our TPF free flyer architecture is unique in its ability to reconfigure the separated spacecraft interferometer or change the interferometer baselines to offer full u-v coverage, and to continue the mission in a lower performance mode if aperture failure occurs. Combiner optics for the structurally connected interferometers nearly matches the design required for the free flyers, except that the free flyer optics may require a voice coil translator whereas the truss architecture does not. We envision differential path length control using thrusters or electromagnets for coarse motion, optical delay lines for medium level control, and fast steering mirrors for fine actuation. The allowable tolerances due to aperture shear, optical path length differences and aperture tilt have been determined, allowing design the optical control system. We have found that controlling optical path differences down to the sub-micron level will be a significant challenge. The science throughput can be increased with fringe tracking while the spacecraft are moving with respect to each other, but the enabling technology needs to be developed.

Propulsion System

Basic selection criteria are generally insensitive to the system layout and specific modes of operation. The on-board propulsion in a structurally connected configuration is envisioned to provide orbit maintenance (*e.g.* solar pressure compensation), initiation and maintenance of baseline rotation, and precision attitude control, or a subset of these functions. In the free flyer configuration, there is the additional requirement to compensate for centrifugal forces acting on each of the collectors. If precision attitude control tasks are accomplished using momentum wheels alone, the thrusters would be fired occasionally for momentum dumping. The thrust levels required for each of these tasks for a generic configuration accommodating baseline dimensions of 10-50 m are summarized in Table 2-7.

Table 2-7. Thrust requirements

	Connected	Free Flyer
Orbit maintenance	1 – 10 mN	0.1 – 1 mN
Formation maintenance		10 – 100 mN
Baseline rotation/momentum dumping	0.1 – 1 mN	0.1 – 1 mN
Precision attitude control	1 – 20 μN	1 – 20 μN

Electric thrusters that can provide relatively high thrust levels between 4 mN and 300 mN are already in existence. For example, Hall Thrusters, have already been demonstrated in ground tests and some of the devices manufactured in the U.S. will be qualified for flight in the near future. Micro-Newton level thrusters, however, are still in their early stages of development, and require additional work.

Among several existing propulsion technologies that can achieve thrust levels in the micro-Newton range, colloidal thrusters are the most promising. They have demonstrated very high efficiency, they operate on non-metallic propellants, which makes them attractive from spacecraft integration standpoint, and they are scalable, i.e. multiple emitters can be assembled into a

multi-thruster array to provide additional thrust over a wide range, as needed, and/or to increase redundancy and improve the reliability of the system. Currently, two laboratory models of colloidal thrusters exist, an integrated system produced by Busek Co. and a flight demonstration model built at Stanford University. Some features of these two systems and their typical performance characteristics (demonstrated in ground tests) are summarized in Table 2-8.

Table 2-8. Characteristics of existing colloidal thruster prototypes

	Busek design	Stanford design
Emitters	Extractor and accelerator grids	Extractor grid only
Voltage	1.8-3.8 kV	2.6-4.4 kV
Thrust	20-189 ?N	100-500 ?N
Array size	57 emitters	100 emitters
Capillary diameter	30 ?m ID, 180 ?m OD	75 ?m ID, 150 ?m OD
Specific Impulse	100-390 sec	50-200 sec
Propellant	Formamide + NaI	Glycerol + NaI
Feed system	Pressurized CO_2, heater activated	Motor-driven syringe
Neutralization	Field-effect cathode	Dual-polarity emission
Subsystem weight	2.5 kg	0.5 kg
Power	6 W	6 W

Thermal Control

The TPF thermal control problem is passive cooling of the collector optics to the temperatures shown in Table 2-9. Thermal models of both the structurally connected and the free flyer configurations were developed to assess the feasibility of meeting these requirements.

Table 2-9. Collector telescope temperature requirements

Baseline (m)	40	21	9	Free Flyer
Collector temperature (K)	40 – 45	40 – 45	60	40 - 45

Structurally Connected Interferometers

A low risk method of achieving the required optics temperatures is to minimize heat sources and provide a large viewfactor from the cooled component to space. This is accomplished in the 40 m structurally connected configuration by placing a long, narrow sunshield far from the telescope truss, as shown in Figure MS-1. As the truss rotates about the line of sight to the target star, the sunshade rotates with it so as to always shade the telescopes, cryostat, and supporting structure from the sun. The sunshield consists of two parallel sheets, spaced to provide significant radiation conductance from the facing surfaces to space. The sun facing surface is a material such as second surface silvered Teflon; all other surfaces are bare vacuum deposited aluminum. Because of the distance between the telescope truss and the spacecraft, conduction from the warm end is minimized.

A thermal model of the 40 m configuration was built using the Cullimore and Ring Thermal Desktop and SINDA codes. Table 2-10 shows the optics and structure temperatures for viewing in the anti sun direction. These were generated assuming worst case optical properties and nominal conduction parameters, with the spacecraft bus maintained at 300K. When viewing at 90? to the sun, the distance between the telescopes and the sunshield varies, but a transient calculation indicates that the optics temperature will be nearly constant, between 16 K and 17 K. These results indicate that the temperature requirements can be met with comfortable margin.

Table 2-10. Steady state optics and structure temperatures for 40 m structurally connected TPF			
Node	Temp (K)	Node	Temp (K)
Collector primary, outer	20	Telescope truss, left	20
Collector primary, inner	22	Telescope truss, center	23
Collector primary, inner	22	Telescope truss, right	21
Collector primary, outer	20	Tower truss, top 1/3	39
Cryostat outer shell	19	Tower truss, center 1/3	73
		Tower truss, bottom 1/3	140

If the temperature requirements are relaxed to 50 – 60 K, the optics can be placed much closer to the sunshield. One approach is to mount the collector telescopes inside a triangular cross section truss, and attach the primary sunshield on the sides of the truss that do not block the telescopes. A secondary sunshield is mounted around each telescope. If the telescopes are completely inside the truss, the telescope array can be pointed anywhere within 90? of the anti sun line, providing 2? instantaneous sky coverage. This eliminates all articulated joints, at great reduction in cost. A model of this configuration gives primary mirror temperatures in the 50 K range, depending on conduction assumptions.

Free Flyer Configurations

We also modeled a free flyer configuration based on that presented in the TPF Monograph. We used a 15 m diameter, 4 layer V-groove sunshield and a cylindrical baffle around the primary, using the same optical properties as above. The optics temperatures in this compact configuration are conduction dominated. The most optimistic assumptions yield a primary mirror temperature of 39K; more realistic parameter values give 80 K.

Cryogenic System

The cryostat requirements for TPF are shown in Table 2-11. The vacuum shell is assumed to be the cooled passively to the same temperature as the collector optics.

Table 2-11. Cryostat Requirements		
Baseline	9-m	21-m, 40-m, or free flyer
Number of Mirrors	2	4
Focal Plane Temperature (K)	< 12	< 7
Focal Plane Power Dissipation (mW)	1 to 5	1 to 5
Spectrometer Temperature (K)	< 17	< 17
Chopper Power Dissipation (mW)	1 to 5	1 to 5
Combiner Temperature (K)	< 60	< 40
Combiner Power Dissipation (mW)	1 to 5	1 to 5
Vacuum Shell Temperature (K)	< 60	< 40
Static Design Loads (g's)	10	10
Minimum First Frequency (Hz)	35	35
Instrument Envelope (Length/diameter, cm)	70/50	88/63
Instrument Mass (spectrometer + combiner, kg)	60	90

Either an active cryocooler or stored cryogens can provide the required instrument and focal plane cooling for TPF. Mechanical cryocoolers have the potential for long operational lifetime (5-10 years) and a lower system mass than stored cryogen systems. JPL's Advance Cryocooler Technology Development Program, scheduled to start in 2002, will develop an engineering model cryocooler by January 2006 that will meet the TPF cooling requirements.

In stored cryogen systems, solid hydrogen is recommended as the primary cryogen, because superfluid helium systems have a larger mass and volume than hydrogen systems. A secondary

cryogen, either solid hydrogen or solid neon, that cools the spectrometer and serves as a guard to the primary cryogen will help to minimize system mass and volume.

Although the combiner temperature requirement is the same as that of the telescopes, and placing it inside the cryostat increases the size and mass of the cryostat, doing so simplifies system alignment and testing, and the components can be maintained at operational temperatures, eliminating any alignment shifts due to thermal cycling.

Trade Studies

Figure 2-9 shows the mass for a SH_2/SH_2 cryostat for the 9 m baseline system (60K vacuum shell), for a range of focal plane (Q_p) and spectrometer (Q_s) heat loads. Using instead SNe as the secondary cryogen increases the system weight but reduces the volume, and the benefits of structural optimization are reduced. For the longer baseline systems, the mass of the cryostat is reduced because of the lower vacuum shell temperature. Again, using SNe as the secondary cryogen increases the system mass slightly.

The mass and envelope of the SH_2/SH_2 system are driven by the heat load to the secondary tank. There is a significant mass savings by using optimized structures with the SH_2/SH_2 cryostat. The additional expense for the design, analysis, and machining of these optimized structures is usually a worthwhile trade-off. The mass of the SNe/SH_2 cryostat is driven by the heat load to the secondary tank, and is largely independent of primary instrument heat load. The mass savings with optimized structure is not as dramatic as with the SH_2/SH_2 system, because the tanks for SNe/SH_2 cryostat are smaller and the secondary cryogen mass is a significant contributor to the total mass. The envelope is independent of instrument heat load because the tanks are relatively small and the envelope is driven by instrument volume. Using solid neon as the secondary cryogen will have a better ground hold performance than using solid hydrogen. The higher thermal capacity of the neon allows longer pre-launch hold without servicing the cryostat.

Comparison with the NGST cryostat, which has similar heat loads and vacuum shell temperature, suggests that employing a warm-launch architecture can potentially reduce the dewar mass. This needs to be traded against the requirements for integration, test, and verification of the instruments.

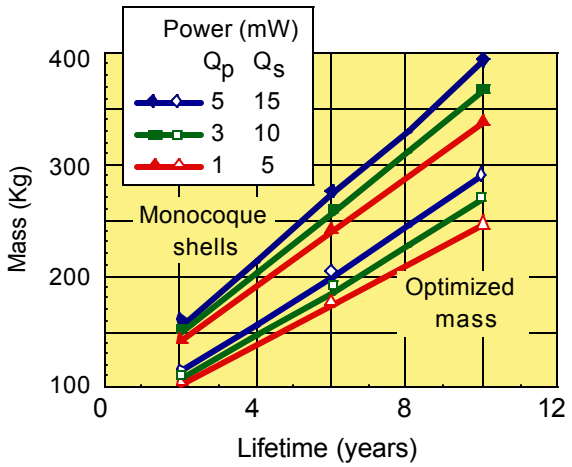

Figure 2-9. Cryostat Mass for the 9-m System. SH_2/SH_2 dewar, 11.5 K/12 K. Instrument envelope 70 cm long x 50 cm diameter. Instrument mass 60 Kg, not included. 60 K vacuum shell temperature

Spacecraft Bus

We evaluated the two existing spacecraft busses for the TPF mission, from IKONOS (LM-900) and SIRTF ("S-Bus"). The evaluation addressed the structurally connected configurations, and identified modifications that would be required. Table 2-12 shows the TPF requirements and capability of the two buses.

Table 2-12. Performance of the candidate buses against the TPF spacecraft requirements

	Capability		Requirements	
	LM-900	S-Bus	9 m	21 m & 40 m
Instrument Power	344 W, 28 V	~64 W	~80W	~64 W
Instrument Mass	470 kg		~1000 - 4000 kg	~400 kg
Pointing Knowledge	10 arcsec	5 arcsec	~10 arcsec	
Pointing Control	12 arcsec	5 arcsec	15 arcsec*	
Pointing Stability	0.8 arcsec/s	0.3 arcsec over 200 s	10 milli-arcsec over 200 Hz*	
Repointing Time	65 sec (2.2 x 1.27 m P/L)	1000 s (SIRTF P/L)	<6 hrs*	
Orbit Maintenance	66 m/s ΔV, 38.4 kg N_2H_4	None	Earth-trailing ΔV = 0 L2 Halo ΔV = TBD	
Instrument Data	Mission specific	1 Mbps peak	24 kbps average*	
Data Storage	Mission specific	16 Gbits BOL	14 Gbits*	
Science Downlink Capacity	Mission specific	2.2 Mbps	400 kbps*	
Mission Design Life	6 years	5 years	>5 years* (10 year goal)	>2.5 years (4 year goal)
Environment	LEO	Earth-trailing	Design for L2 halo or Earth-trailing*	
* Denotes value from the TPF Monograph.				

Bus Modifications Required

The Lockheed Martin LM900 is a 3 axis stabilized spacecraft bus that is derived from the IKONOS 1-meter imaging satellite. The S-Bus is derived from the spacecraft developed for the SIRTF observatory. The SIRTF spacecraft was itself derived from the series of Mars orbiter and lander spacecraft, and this extensive heritage provides a wealth of equipment options that can be used to adapt the core bus architecture to TPF.

Both buses require similar modifications to accommodate TPF mission requirements:

- Replace body mounted solar panels with deployable sun-tracking arrays.
- Modify ACS to use instrument steering sensor input. This is similar to the HST Fine Guidance Sensor.
- Revise bus thermal control radiator and insulation details as required to meet equipment requirements and attitude constraints
- Update FSW to provide payload/mission support, solar array deployment and tracking
- Modify the bus interface controls to accommodate science data, telescope, light path, and combiner controls, temperature monitors, deployment mechanisms, and telescope and combiner electronics.
- The S-Bus also requires upgrading of the cold gas propulsion system.

The TPF interferometer will also include features that define the spacecraft interface requirements:

- Telescope controls
  - Secondary mirror focus mechanism – Linear position adjustment with position measurement, set and forget

- ? Tertiary mirror fast steering motor – two axis piezo-electric drive, range 30–60 arc sec, control drive rate 20 Hz (Discussed SIRTF CDMU as possible design candidate)
- ? Temperature monitors

?? Light path controls
- ? "Trombone" linear actuator – 100 nm control range, periodic adjustment

?? Combiner controls (inside cryostat)
- ? Fine phase adjustment – Linear actuator, phase detection 200 Hz, drive rate >20 Hz, processing logic and latency estimates
- ? Alternating chopper mirror – dual or coupled motors driven from single mechanism. Position feedback, dynamic actuation at ~4 - 0.25 Hz. (Discussed SIRTF MPS scan mirror drive electronics as possible design candidate)

?? Detector controls (inside cryostat)
- ? IR detector array – Single large array sufficient for both images. Primary science data
- ? Near IR detector arrays for fine phase measurement, read at 200 Hz
- ? Two quad cell arrays - For telescope fine pointing, read at 200 Hz, closed loop control with telescope tertiary fast steering mirrors, drive at 20 Hz.

?? Cryostat controls
- ? Vent valve – single pyro-actuation type
- ? Low temperature monitors (~12)

?? Deployment, slewing, and rotation controls
- ? Hold-down and release mechanisms
- ? Telescope truss rotation drive mechanism or μN thruster
- ? Other motors, actuators, and mechanisms not defined
- ? Measurements and sensors, not defined

Bus modifications required to accommodate the interferometer include new electronics boxes, as described in Table 2-13.

Table 2-13. Warm Electronics to Interface to TPF Payload

Payload Telescope Controls Electronics (PLTC)	Payload Combiner Controls Electronics (PLCC)
Secondary Focus Drive Electronics	Chopper Motor Drive Electronics
Tertiary Fast Steering Mirror Drive Electronics	Infrared Detector Data Handling Electronics
Trombone Path Length Adjust Drive Electronics	Near Infrared Phase Detector Electronics
Quad Cell Detector Processing Electronics	Phase Adjustment Control and Processing
Cryogenic Temperature Interface Electronics	Fine Phase Adjust Drive Electronics
Attitude Control System Interface to S/C	Science Data Handling Interface

Interfaces currently not required include telescope dust covers light aperture doors, with their associated drive motors and sensors, additional cryo control logic, mechanisms, flow rate and pressure measurements, laser structural alignment system, additional spectrometer controls, and an amplitude balancing system.

Mass and Power Summary

An rough estimate of the mass and power required by the various spacecraft subsystems and instrument components is shown in Tables 2-14. These include the above modifications.

Table 2-14. Structurally connected interferometer TPF mass and power summary for two LMMS spacecraft buses								
	Weight (Kg)				Power (W)			
TPF Configuration	40 m SCF		9 m SCF		40 m SCF		9 m SCF	
SC Bus	LM900	S-Bus	LM900	S-Bus	LM900	S-Bus	LM900	S-Bus
Telescopes	600	600	79	79	0	0	0	0
Cryostat	270	270	150	150	0	0	0	0
Beam combiner	90	90	60	60	0	0	0	0
Instrument electronics	29	29	29	29	80	80	64	64
Truss structure	456	456	49	49	0	0	0	0
Tower	40	40	10	10	0	0	0	0
Sunshield	1818	188	15	15	0	0	0	0
Instrument total	**1673**	**1673**	**392**	**392**	**80**	**80**	**64**	**64**
Structures & mechanisms	205	145	171	121	12	12	12	12
Thermal control	38	44	38	44	24	24	24	24
Attitude control	86	81	86	54	114	193	114	69
Communications	222	26	22	26	43	33	43	33
Command & data handling	55	23	55	23	105	66	105	66
Electrical power	87	120	87	111				
Battery charging					18	18	18	18
Cable losses					6	9	6	6
Propulsion	22	22	12	12	2	2	1	1
Spacecraft total (dry)	**515**	**462**	**470**	**390**	**325**	**383**	**323**	**256**
Observatory total (dry)	**2189**	**2135**	**862**	**782**	**405**	**463**	**387**	**320**
Propellant	96	96	38	38				
Observatory total (wet)	**2285**	**2232**	**900**	**820**				
Power capability (EOL)					681	574	681	396
Atlas V 401 capab. (w/adapter)	3306	3291	3306	3291				
Margin	**45%**	**47%**	**267%**	**301%**	**68%**	**24%**	**76%**	**24%**

Orbit Selection

The significant effects are in the communications and propulsion subsystems. In the Earth trailing orbit, communications system needs to be designed for a wide range of data rates to accommodate the increasing range. The S-Bus has been designed for this orbit, and the same or similar communications hardware can adapted to the LM-900 bus.

The L2 Halo orbit requires propulsion to maintain orbit. The LM-900 bus already has sufficient propulsion for the SPF configuration, but may need to be upgraded for the larger configurations. The existing S-Bus propulsion is wholly inadequate, and would need to be enlarged or replaced to manage solar torques for either orbit.

A launch vehicle capability analysis, depicted in Table 2-15, shows that the payload mass capability for launch into the SIRTF-type drift-away orbit is slightly less than that for launch into the L2 orbit. Note that the higher mass capability for the L2 orbits is offset by the ?V required for stationkeeping near the unstable Lagrangian Point.

Table 2-15. Payload mass capability (kg) for launch of TPF into 1 AU orbits			
Launch Vehicle	L2 Halo, Lunar swingby	L2 Halo, Direct	1 AU Drift-Away
Ariane 5	6200	5970	5810
Delta III	2770	2700	2650
Delta IV Med	2820	2750	2700
Delta IV Med + (5,2)	4150	4060	4000
Delta IV Med + (4,2)	4450	4360	4300
Delta IV Med + (5,4)	4750	4660	4600
Delta IV Heavy	10400	10090	9880
Atlas V 501	2820	2760	2710
Atlas IIIB	3400	3310	3240
Atlas V 401	3600	3510	3440
Proton M Breeze M	4910	4820	4760
Atlas V 551	6620	6420	6280

Integration and Test

The guiding principles are incremental performance verification, early interface testing on all major components using simulators and testbeds, and maximum utilization of existing and COTS hardware and equipment. All essential or risk elements are modeled, characterized, and validated before entering the manufacturing and test phases. Program elements with low technology readiness levels will undergo test flows as shown in Figure 2-10. All other low risk components will be verified through the protoqual test program where each component/subsystem is functionally and environmentally validated prior to the next level of verification.

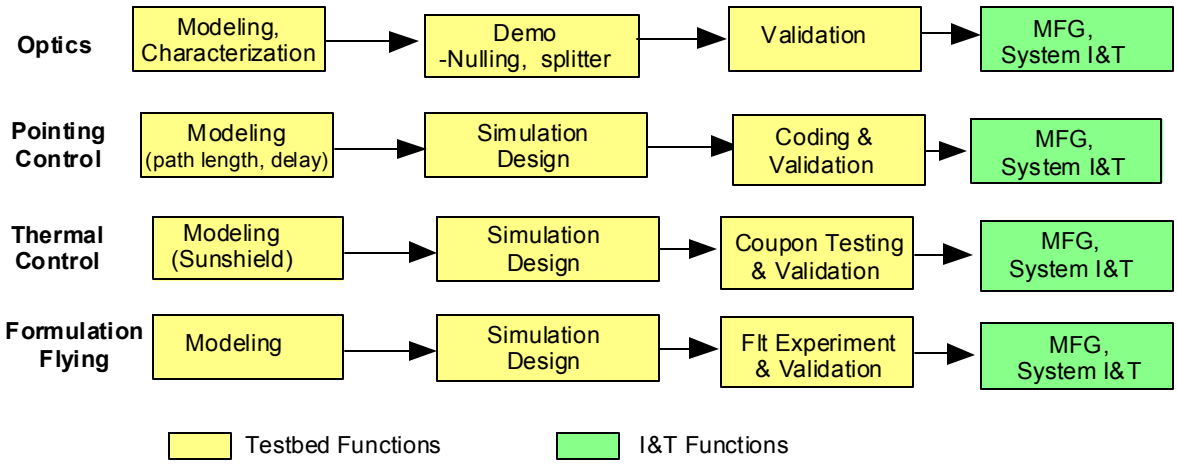

Figure 2-10. Key TPF Elements are Full Validated Prior to the System Level I&T

Thermal vacuum testing of the integrated 40m system in the LMMS Delta chamber is shown conceptually in Figure 2-11. The objectives of this test that structural distortion and optical path length control meet requirements. The combiner optical performance will have been demonstrated at the cryostat prior to the Observatory level thermal vacuum test.

The Delta TV chamber is a 24 m long, 10m diameter horizontal cylinder. For the 40 m structurally connected TPF, half of the 40m telescope truss with 2 collectors and the cryostat can be fully deployed in this chamber. An optical "wing simulator" can be used to simulate the missing collectors. Repeating the test with the other wing validates the complete assembly in a piecemeal fashion. Optical alignment performed before and after the TV test will verify that structural and optical integrity are maintained.

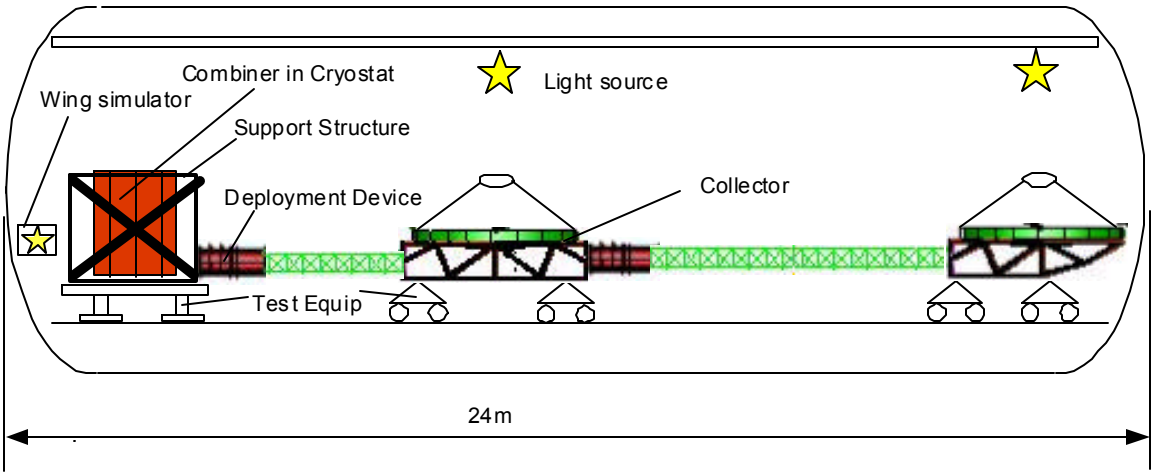

Figure 2-11. 40 m structurally connected TPF thermal vacuum test concept

Existing, co-locate test facilities on the LMSSC Sunnyvale campus are available for TPF final integration and testing. The facilities include a 17x36x27 m high Class 10K clean room with a 20 ton bridge crane at 23 m hook height, a 12x15x26 m high acoustic cell (Figure IT-2) adjacent to the high bay, and a dual entry 12 m diameter, 24 m long horizontal thermal vacuum (T/V) chamber (Figure 2-12).

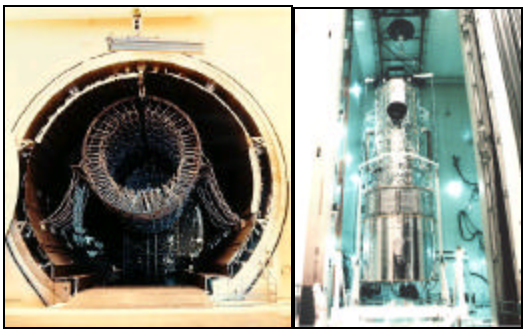

Figure 2-12. Delta thermal vacuum chamber with IR light cage and HST in acoustic cell

Orbits and Sky Coverage

Earlier TPF studies investigated four candidate orbits for the TPF mission: a 5 AU radius solar orbit, a 1 AU x 3 AU solar orbitl, a 1-AU "drift-away" solar orbit, and a "halo" orbit about the sun-earth Lagrangian Point L2. This work led to the preference by the science members of the Lockheed Martin team for the 1 AU orbits, i.e., drift-away or L2.

Because the earth blocks 85% of the sun at the L2 point itself, this feature could be exploited to reduce cooling requirements. However, this must be traded against the need for larger solar arrays, communications uplink interference from the sun, and propulsion required to keep the observatory in the earth's penumbral core which moves laterally with the earth-moon barycenter by up to ?4670 km over 29.5 days. Stationkeeping maneuvers totaling on the order of 16 km/sec per year would be required to maintain, say, a 75% - 85% occultation level near the L2 point. Similarly, placing the observatory completely in the umbra ~100,000 km closer to the earth promises further reduction in optics cooling requirements, but power is a problem. Power beamed (via microwave or otherwise) from a companion spacecraft orbiting in sunlight is a possible approach, but the technology is not ready ? accommodating inefficiencies at the collec-

tion point must be weighed against the difficulty of shielding from the sun. A nuclear isotope power option would introduce entirely different considerations. The LMSSC team does not recommend utilization of earth-shadowed orbits for foreseeable TPF missions.

Sky coverage is conveniently discussed in terms of the angle between the viewing direction and the anti-sun line. If viewing is permitted anywhere within 45? of the anti-sun line, i.e., if the sun exclusion angle is 135?, 15% of the sky is visible at any one time, Because the observatory at 1 AU completes a revolution of the sun in one year, the accessibility cone sweeps out a swath along the ecliptic during the year that encompasses 71% of the sky. The 29% of the sky within 45° of the ecliptic poles is permanently inaccessible with this constraint. A given target on the ecliptic is accessible continuously for about 91 days in this case (25% of the year), but then becomes inaccessible for about 9 months. Targets off the ecliptic are available for shorter periods, separated by a greater length of time. Table 2-16 shows this accessibility for other values of the anti-sun constraint angle.

Table 2-16. Dependence of sky coverage on anti-sun constraint angle

Anti-sun constraint angle	45?	90?	135?
Percentage of sky accessible at any time	15%	50%	85%
Percentage of sky accessible over 1 year	71%	100%	100%
Number of consecutive days a given target ecliptic is accessible	91	183	274

Of the 259 sample targets on the list developed by D. Ebbets and distributed by the TPF Science Working Group, a spacecraft limited to viewing only within 45? of the anti-solar direction would be able to access only 180 of these targets, because 79 are at higher ecliptic latitudes than ?45?. In addition to geometric constraints on TPF viewing in certain sky directions, there may be viewing constraints imposed due to the presence of copious background objects, such as Milky Way galaxy stars which may crowd even the small fields of view of interferometers. Imposing the additional constraint that target stars must lie more than 10? from the galactic plane to avoid this background confusion eliminates another 31 stars from the sample list.

Scientists on our team have long considered adequate sky access to be a critical factor in the design of a TPF observatory. All of the structurally connected interferometer configurations in our baseline approach allow viewing anywhere within 90? of the anti-sun line, and thus provide 100% sky coverage in the course of a year.

30-Day Reference Mission Profile

Section 5.2.1 summarizes our TPF Reference Mission Analysis for the baseline 40-m design configuration, which is contained in a separate document. We have utilized the performance results of that analysis to begin preparing preliminary high-level timelines for use in mission planning studies and as an engineering design reference. Figure 2-13 depicts a typical 30-day mission profile representative of the second year of operation in the 1-AU drift-away orbit: a relatively mature phase when the planet detection survey (including repeat visits) still occupies half of the schedule, but medium-depth spectroscopy is also occurring in order to characterize suspected terrestrial planets, and deep spectroscopy has been begun to search for the presence of biomarkers for the most promising candidate planets.

For the timeline it is assumed that onboard data storage sufficient for 3 days' operation is available, but that in general daily science data downlink contacts of about one hour are scheduled except during longer science exposures. Dumping of excess angular momentum using thrusters

is performed at least every 1-1/2 days, simultaneous with data downlinking where possible. It is also assumed that a suite of optical and spacecraft calibrations, as yet not fully defined, is performed every two weeks and before extremely long integrations; these data are sent to the ground immediately. Planet detection, astrophysical imaging, and planetary spectroscopy programs are shown occurring in blocks.

The inset to the figure shows a time allocation breakdown of on-orbit activities for the 30 days. The small number of target-to-target slews and long integration times result in high observing time efficiency. Experiment setup time is significantly shorter for the structurally connected configuration compared to a free-flying configuration, for which vehicle and beam alignment procedures are considerably more complex.

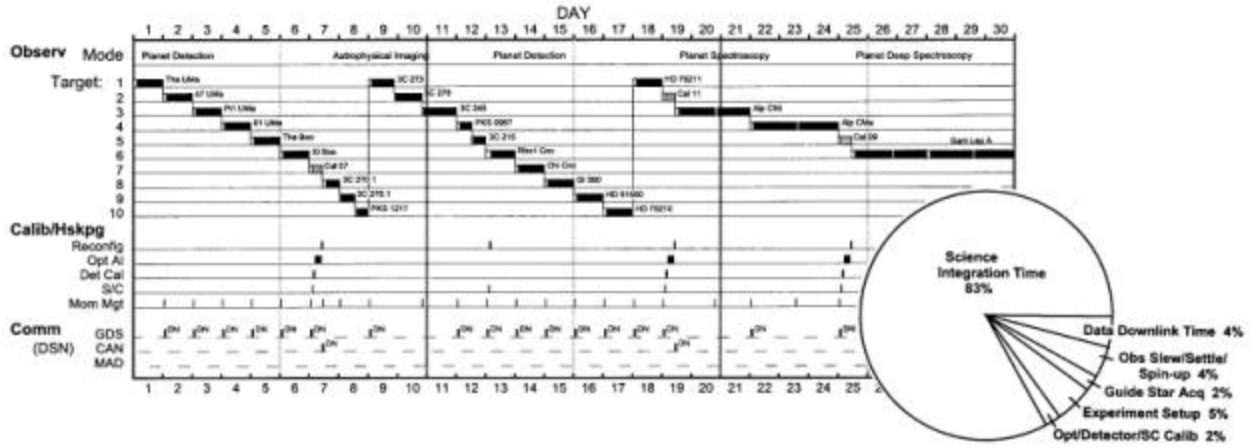

Figure 2-13. Typical 30-Day TPF Reference Mission Profile and Time Breakdown

Flight Operations

The TPF Ground System organization shown in Figure 2-14 is based on the SIRTF ground system design, with minor modifications drawn from lessons learned from SIRTF. The ground system is divided into two main organizations, the Mission Operations System (MOS) and the TPF Science Center (TSC). The TPF MOS is responsible for similar functions as the SIRTF FOS - namely, the day-to-day operations of the observatory and observatory health and status. The TSC is responsible for the TPF science program (selection of TPF science and preparation of observation requests), as well as education/outreach and community (astronomy) support.

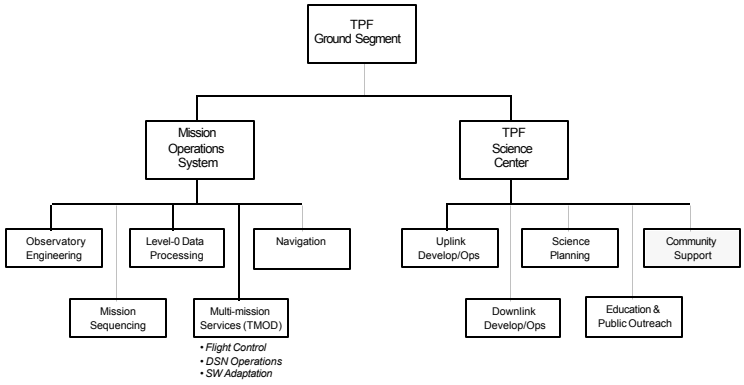

Figure 2-14. TPF Ground System Organization

The TPF MOS is composed of six teams: Systems Engineering, Observatory Engineering, Mission Sequencing, Level-0 Data Processing, Navigation, and Multi-Mission Services. JPL is presumed to be responsible for the TPF MOS, and the teams that make up the MOS are either JPL or contractor employees. The TSC is composed of five teams: Systems Engineering, Science Planning and Community Support, Uplink Development/Operations, Downlink Development/Operations, and Education and Public Outreach (E&PO). Following SIRTF, responsibility for implementing the TSC is presumed to be with IPAC at Caltech. All TSC teams are presumed to be Caltech employees.

The TPF ground data system is envisioned to be similar to SIRTF, as shown in Figure 2-15. Unlike SIRTF, TPF would only require once per day downlinks, and therefore only require use of a single DSN station.

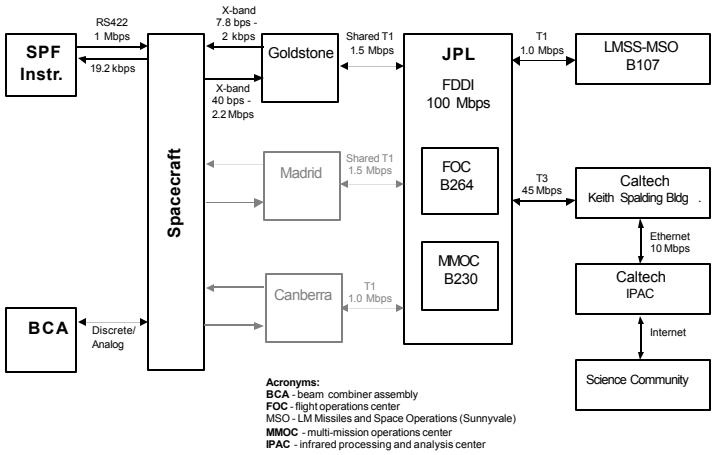

Figure 2-15. TPF Data System

5.1.1.2 Planet Detection Capabilities

Input coming

5.1.1.3 Astrophysics Capabilities

Input coming

5.1.1.4 Mission Feasibility

In this section, we address the TPF mission schedule, cost, and technology development requirements.

Mission Schedule

Our TPF program approach is based on a phased incremental development that provides for launch of a full-scale TPF observatory in October, 2013, as shown in Figure 2-16. This allows early experience with structurally connected nulling IR interferometer observations of young Jupiters, followed by the capability to observe earth-like planets out to 12 or 22 pc, and ozone, water, and carbon dioxide to 8 or 15 pc for 21 and 40 m baseline instruments, respectively. This includes development of a 9 meter baseline Structurally Connected Interferometer (SCI) precursor starting in the 4th quarter of 2002 for launch in 2006. The 40 meter full-scale SCI that meets

all Exhibit 2 planetary detection and characterization science requirements is initiated in 2007, after a year of on-orbit technology demonstration by the precursor, and launched in 2013. Alternatively, a 21 meter SCI could be launched in lieu of the 40 meter system to facilitate budget restrictions. This would also provide additional time for technology development for a Free Flyer interferometer in place of a larger SCI.

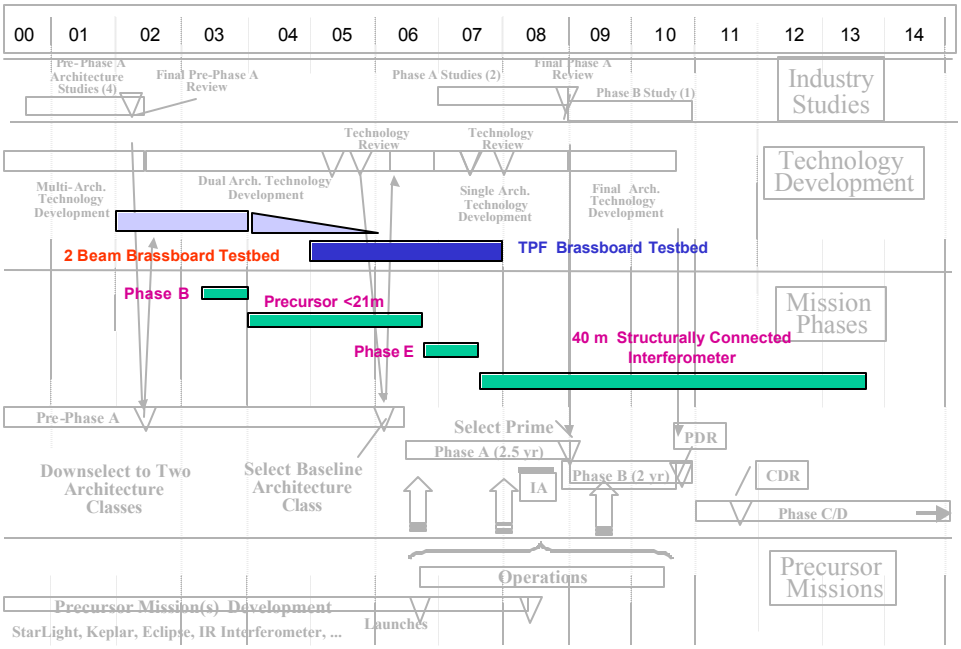

Figure 2-16. Incremental development plan for TPF and comparison with JPL phasing plan of December 2001.

We also prepared a series of program schedules for each of the structurally connected interferometer options. These schedules include all flight and ground elements of the TPF system (except the Launch Vehicle). Program management, system engineering, design engineering, optics system integration, fabrication, assembly, integration and test are accomplished at LMSSC in Sunnyvale and Palo Alto. Mirror development, fabrication and testing are performed at University of Arizona Steward Lab.

Cost

The LMT developed cost data both through estimates by key team personnel and parametrically by MIT using the GINA program. The program schedules shown above provided a time basis for determining costs. The cost estimates for the three SCI configurations are summarized at the element level (Spacecraft & Truss, Optical System, Launch Vehicle, Operations) and shown in Table 2-17. Totals include a 30% contingency. Spacecraft costs are based on modification of existing LM Ikonos and SIRTF spacecraft buses. Operations costs are consistent with planned SIRTF mission operations software, hardware and staffing plans. Launch Vehicle costs are based on CY 2001 data.

Table 2-17. Structurally connected interferometer TPF cost summary				
Baseline	40 m	21 m	18 m	9 m
Spacecraft and truss system	$304M	$173M	$120M	$98M
Optical system	$558M	$168M	$82M	$47M
Launch vehicle	$120M	$100M	$75M	$75M
Phase E/Science	$500M	$300M	$40M	$30M
Totals (with 30% contingency)	$1741M	$843M	$390M	$293M

Technology Readiness

Table 2-18 shows a summary technology status matrix, in terms of current and required metrics, TRL, and the degree of difficulty, mission impact, and probability of achieving TRL = 9 in the TPF timeframe.

Overview

Collector telescope optics TRL is high for 0.6 m aperture diffraction limited at 2 ?m, but development is required for larger apertures. Optical path length errors, transmission asymmetries, and differential polarization have been addressed in the SIM testbed and in Serabyn's test lab, but development is required to bring the technology to the readiness level required. The MMZ Nulling Beam Combiner is an extension of the BLINC beam combiner, but the TRL of dielectric phase plates and symmetric beam splitters is low. The basic spacecraft ACS is mature and flight proven. The use of tuned mass dampers to achieve system level damping has been demonstrated in simulation and requires hardware demonstration at the proper environment. Pointing jitter control using detector signals in a feedback loop to drive a fast steering mirror is a mature concept, but operation and performance at cryogenic temperatures should be demonstrated. The risk associated with these technologies is considered low. Active path-length control using feedback signals from a fringe tracking system and an active delay line is the control system technology requiring most development. This is due to the unique approach for phase detection, which has been demonstrated in a ground telescope, but needs to be demonstrated in an active closed-loop system, followed by demonstration in the proper environment. The risk associated with this technology is considered moderate. Deployable structure for support of the 21 m and 40 m baseline interferometer components relies on mature technologies, the principal risk being in meeting alignment requirements. We rely on sunshields to for passive cooling of the optics, cryostat outer shell, and supporting structure. The sunshield components use flight proven materials systems; the risk is in validation testing because of the sunshield size and environment temperature requirements. TPF formation flying will be enabled through the development and deployment of automated space borne guidance, navigation and control systems integrated with intra-satellite communication infrastructure. These technology drivers are identified in Table TR-1.

Testbeds

We are proceeding with an optics testbed for development of beam combiner technologies, starting with a brassboard 2-beam combiner under IR&D funding in 2002-03. A system level control technologies testbed is also proposed to identify and resolve system issues, support model development and validation, and demonstrate integrated operation and the approach for pointing and path-length compensation. The roadmap for free flying technology development includes two and three dimensional ground testbeds, followed by on-orbit experiments to demonstrate multi-vehicle control and drift-through fringe tracking, and transition to real science missions.

Table 2-18. Lockheed Martin Team TPF Technology Status						
Technology Element	Mnow	Mreq	TRL	DegDiff	Impact	Probability
Modified Mach-Zender Nulling Beam Combiner (Mnow from Bracewell IR Nulling Cryostat)						
Deepest Null Capability (reflects sum of all issues below)	10^-4 IR mono, 10^-6 vis mono, not sustained	3x10^-5 broad-band	3	70	60	80%
Gold entrance mirrors (dichroic quaternaries)	IR ground telescopes		6	10	85	100%
2 µm phase detector	BLINC lab test, due at telescope spring 2002		6	15	100	98%
Dielectric Phase Plates	Single plate	Two plates	3	60	75	85%
Symmetric Beamsplitters	Mach-Zender standard in lab	IR implementa-tion	3	20	85	98%
Vibration mitigation, pointing, and path length control						
Damping	Not demonstrated at sys level	0.1% damping	4	30	75	95%
Active jitter compensation (fast steering mirrors)	Adequate at room temp	Need demon-stration at cryo	3~4	20	100	95%
Coarse "Trombone" path length adjust	SIM (1 m throw w/ 1 mm res; not cryo) SIRTF actuater	~100 nm range	4	30	75	95%
PZT (fine path length adjust)	BLINC	~1nm	6	40	100	95%
Fringe tracking	BLINC	2 nm	4	70	100	60%
Raw pathlength error budget	84 nm rms (simulation)	84 nm rms	3	60	25	60%
Compensated pathlength allowable error	1.2 nm rms (analysis)	3.6 nm rms	3	70	100	60%